

Energy Advances

Accepted Manuscript

This article can be cited before page numbers have been issued, to do this please use: A. A. Altalhi, E. A. Mohamed and N. A. Negm, *Energy Adv.*, 2024, DOI: 10.1039/D4YA00272E.



This is an Accepted Manuscript, which has been through the Royal Society of Chemistry peer review process and has been accepted for publication.

Accepted Manuscripts are published online shortly after acceptance, before technical editing, formatting and proof reading. Using this free service, authors can make their results available to the community, in citable form, before we publish the edited article. We will replace this Accepted Manuscript with the edited and formatted Advance Article as soon as it is available.

You can find more information about Accepted Manuscripts in the [Information for Authors](#).

Please note that technical editing may introduce minor changes to the text and/or graphics, which may alter content. The journal's standard [Terms & Conditions](#) and the [Ethical guidelines](#) still apply. In no event shall the Royal Society of Chemistry be held responsible for any errors or omissions in this Accepted Manuscript or any consequences arising from the use of any information it contains.

Recent advances in layered double hydroxides (LDH)-based materials: Fabrications, modification strategies, characterization, promising environmental catalytic applications, and prospective aspects

Amal A. Altalhi¹, Eslam A. Mohamed^{2#}, Nabel A. Negm^{2#}

1- Department of Chemistry, College of Science, Taif University, P.O. Box 11099, Taif 21944, Saudi Arabia

2 - Egyptian Petroleum Research Institute, Nasr City, Cairo, Egypt.

Corresponding authors: eslamepri@gmail.com (Eslam. A. Mohamed); nabelnegm@hotmail.com (Nabel A. Negm)

Abstract

Layered double hydroxides (LDHs) are clay networks with brucite ($\text{Mg}(\text{OH})_2$) layers that are coupled with anion between the produced layers. The building structure of LDHs follows the formula: $[\text{M}^{2+}_{1-x}\text{M}^{3+}_x(\text{OH})_2]^{x+}(\text{A}^{n-})_{x/n} \cdot y\text{H}_2\text{O}$, where M^{3+} and M^{2+} are trivalent and divalent cations in the structural units (sheets), x is the structure's M^{3+} to $(\text{M}^{2+}+\text{M}^{3+})$ cation ratio, and A^n is the interlayer anion. LDHs can be created utilizing simple approaches that regulate the layer structure, chemical composition, and shape of the crystals generated by adapting the production parameters. The first method of modifying LDH composites is through intercalation, which involves inserting inorganic or organic precursors into its composition, which can then be employed for a variety of purposes. The next method is a simple physical mixing technique among the created LDHs as well as advanced materials such as activated carbon, graphene and its derivatives, and carbon nanotube to be utilized as base substances in energy storage, supercapacitors, photo- and electrocatalysts, water splitting, and toxic gas removal from the surrounding environment. The final strategy is the synthesis of polymer-LDH composites by inserting effective polymers during the manufacturing process of LDHs to create nano-composites utilized for energy, fire retardant, gas barrier, and wastewater cleaning. LDHs are a sort of fine chemical that can be designed to have the desired chemical structure and performance for usage in a variety of purposes such as redox reaction, the process of bromination, ethoxylation, aldol condensation, NO_x and SO_x elimination, as well as biofuel production. Because LDH substances are not harmful to the environment, the different applications that use them are unique in terms of green chemistry because they are recyclable and eco-friendly catalysts. The present review investigated the various methods used to create LDHs and the improvement of the produced composites by enhanced temperature calcination, intercalation of their structures by small-, medium-, and high-nuclear anions, and support by carbon compounds. The evaluation methods as well as the best prospective uses, such as biofuel generation, catalysis, water splitting, charge transfer, and wastewater treatment, were comprehensively reported according to the most current studies, and the potential sight of LDHs is highlighted.



Keywords: LDH; Catalysis; biofuel production; Flame retardance; wastewater treatment

View Article Online
DOI: 10.1039/D4YA00272E

1. Introduction

Layered double hydroxides (LDHs) are made up of two metal cations; divalent and trivalent in the form of double layers or lamellar structures. Anions (nitrates, sulfates, or carbonates) and water molecules are essentially filling the interlayer gaps between the metal hydroxide layers.¹⁻³ The general formula for LDHs $[M^{2+}_{1-x}M^{3+}_x(OH)_2]^{x+}(A^{n-})_{x/n} \cdot yH_2O$, where M^{2+} and M^{3+} are the divalent and trivalent metal cations, A^{n-} is the related anion, and x is the ratio of $M^{3+}/(M^{2+} + M^{3+})$ where $(0.1 < x < 0.5)$. Furthermore, the M^{2+}/M^{3+} ratio must be in the 1-6 range⁴⁻⁶ to produce LDHs. From an organizational standpoint, LDHs come from brucite, or mineral clay, which is mostly made of $Mg(OH)_2$. An equivalent amount of trivalent metal cations (M^{3+}) replaces a portion of the divalent metal cations (M^{2+}) during the production of LDH based on brucite. As a result, there are positive charges left on the layers' surface, which are balanced by water molecules and comparable anions that occupy the interspace among the layers. The assembly of the lamellae and formation of the distinctive LDH structures are supported by the anions' compensation of the generated positive charges⁷. The hydroxide layers are contained in the cores of octahedral structures (**Figure 1**), and the cations M^{2+} and M^{3+} are uniformly distributed throughout the lamellar structures^{6,8}.

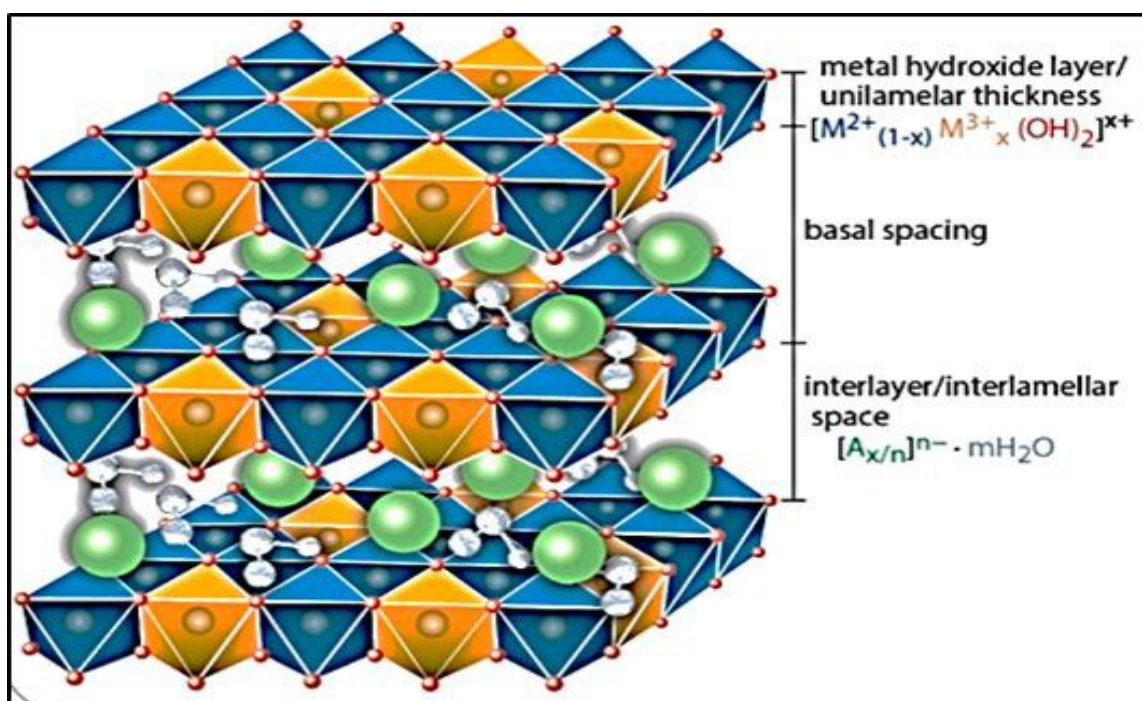


Figure 1: The layered double hydroxides' distinctive gaps and distances.

The LDH structures are stabilized due to the electrostatic interaction among the positive charge layers and the negative charge anions present amongst these layers. The density of the remaining positively charged layers and the number of negative charge anions connected to



the construction can be established by the ratio among the M^{2+} and M^{3+} cations in the framework of the LDH layers. The valence of the cations and the relationship between the different ion types significantly affect the layered double hydroxide characteristics, particularly their porosity, ion exchange propensity, and crystallinity ⁹.

2. Techniques applied for LDH preparation

Different techniques are used to create layered double hydroxides. Every technique may provide a distinctive product with certain characteristics, mostly in terms of surface area, shape, crystallinity, and physical and chemical characteristics. The co-precipitation technique, hydrothermal approach, and sol-gel technique are the most often used techniques for creating layered double hydroxides.

2.1 Method of co-precipitation

The most popular technique for creating double hydroxides is co-precipitation. This involves vigorously spinning diluted solutions of metal cation salts at certain temperatures between 50 and 90 °C ^{10–12}. Then, employing NaOH or NH₄OH in the existence of a perfectly appropriate concentration of carbonate salt in the form of Na₂CO₃, the medium's pH is changed to alkaline, precipitating the produced metal oxides. The reaction time and the alkalinity of the medium have the ultimate impact on the creation of the layered double hydroxides. At a pH of 9–12, for 24 hours under stirring conditions and drop-wise titration, improve the shape, surface area, and crystallinity of the resulting layered double hydroxides ¹³. However, this methodology results in the combination of counter hydroxide ions in/on the inter-outer layers of LDH ¹⁴. The co-precipitation method offers numerous advantages, comprising a high yield, one-step synthesis, crystalline LDHs, and high purity ¹⁵.

2.2 The hydrothermal approach

The layered double hydroxides are prepared using the hydrothermal technique at temperatures as high as 180 °C and under pressure. The production environments, such as: temperature and time of the hydrothermal process play a vital role in defining the crystallinity of the prepared LDHs. The hydrothermal technique is predominantly appropriate when foreign organo-anions with low-affinity needed to be assimilated in the prepared LDHs interlayers. The hydrothermal technique compromises several advantages, e.g., controlled particle dimensions, morphology, and the presence of only hydroxide anions in the crystal lattices ¹⁶. This procedure may be used for the initial reactants or after the metal cation mixing ¹⁷. Sharp crystals and a large surface area are characterized by the layered double hydroxides that are produced when hydrothermal procedures are used at higher temperatures.

2.3 The Sol-Gel technique



Sol-gel approach includes the occasionally employment of acetates and acetyl acetonates as anions. The anion salts are disseminated in an organic solvent and the hydrolysis of the alkoxides is operated to obtain a sol matrix. Then mixing of the medium creates the required LDHS which resulted from the colloidal phase gel that formed due to internal cross-linking. The characteristics of the resulted LDH are frequently improved by amending the condensation rate, pH, temperature, and solvent type metallic precursors during the hydrolysis. The produced LDHs via sol-gel approach had high purity, a large surface-area, and precise pore-size^{18,19}.

In comparison between the different routes, the most famous routes used for preparation of LDHs are: co-precipitation, hydrothermal, and sol-gel. There are several advantages and disadvantages were reported for the obtained products within these methods. Co-precipitation route involves simple stages and equipment, with economical, rapid, and scalable LDH yields. But, the obtained LDHs lack of effective control in the crystallinity and lattice arrangement. The hydrothermal route is used for a large-scale production of LDHs with effective controlling of the crystallinity and morphology, with longer time of reaction and higher energy. The sol-gel route permits the preparation of either nanostructured characterized by high crystallinity and regular morphology after long reaction time, while powder LDHs with low crystallinity at short reaction time²⁰.

3. Calcination of layer double hydroxides

Layered double hydroxides are undergoing a lamellar structural reorganization at high temperatures due to the calcination process. Mixed metal oxides are created as a result of this process, which enhances the formation of the octahedral to the tetrahedral crystalline structure of LDH. More positively charged cations are formed due to this process as a result of the defects formed in the crystalline structures. The creation of defects in the produced crystalline structures serves as compensation for these charges. These defects include the presence of oxygen in the structure and cationic vacancies²¹⁻²⁴. To produce the matching 3-D framework of diverse metal oxides (**Figure 2**)²⁵, three different kinds of reactions took place through the calcination of LDHs: the first reaction is the dehydration of adsorbed and interlayer water molecules, then dehydroxylation of the layers, followed by the decomposition of the anions.



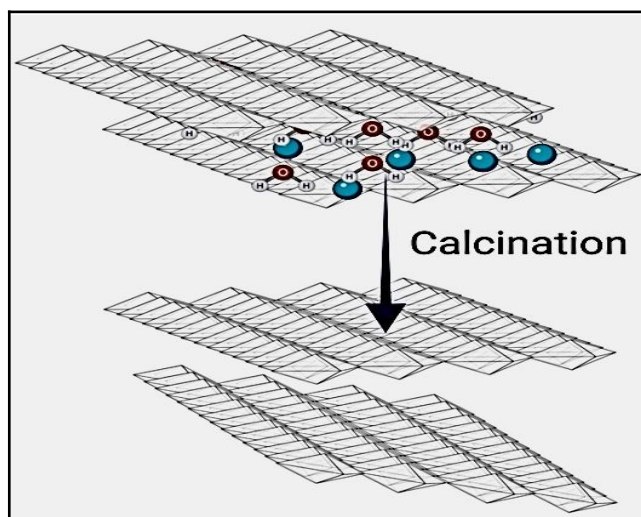


Figure 2: Mixed metal oxides in a 3-D LDH network.

4. Physicochemical methods of LDH characterization

Several methods are often used to study layered double hydroxides, including Fourier transforms infrared spectroscopy (FTIR), X-ray photoelectron spectroscopy (XPS), scanning electron microscopy (SEM), X-ray diffraction (XRD), and thermogravimetric analysis (TGA).

4.1 XRD spectroscopy

The most important spectroscopic technique for figuring out the created LDHs' degree of crystallinity, the arrangement of the generated layers, and the gaps between them is their XRD diffraction profile. Each LDH has a unique fingerprint that reveals its crystalline and geometrical arrangement, which may be interpreted as a sign of the structure's acceptable quality and purity. JCPDS file no. 22-700 identifies the distinctive sharp, thin, and symmetric reflections relevant to low values of 2-theta (θ) of typical basal planes (003), (006), and (009), of the hydrotalcite structure²⁶. Moreover, it demonstrated the emergence of wide and asymmetric reflections at the 2-theta of the non-basal (012), (015), and (018) planes (**Figure 3**). Regardless of the production process, the characteristic 2-theta values of the various LDHs remain constant, while the variation is found in the d -spacing between the LDH layers, which is determined by the size and kind of intercalated ions that exist among the layers.



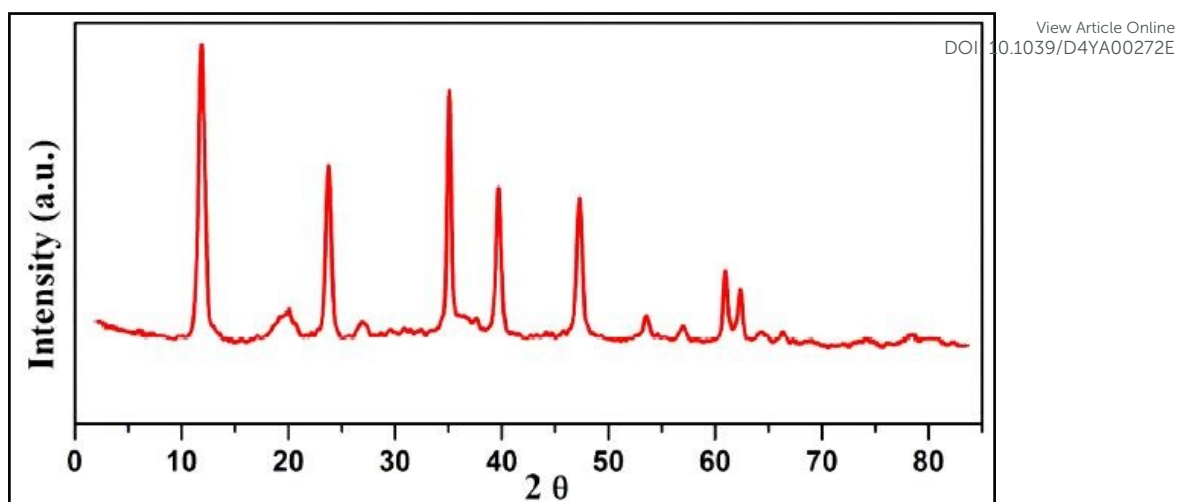


Figure 3: X-ray diffraction patterns of NiMo/LDH.

4.2 SEM analysis

Scanning electron microscopy (SEM) is useful for imaging the hydrotalcite structural unit of the LDH framework (**Figure 4**). Highly porous plate-like crystalline arrangements in a hexagonal-ordered crystal structure are often seen in the SEM pictures of layered double hydroxides ²⁶.

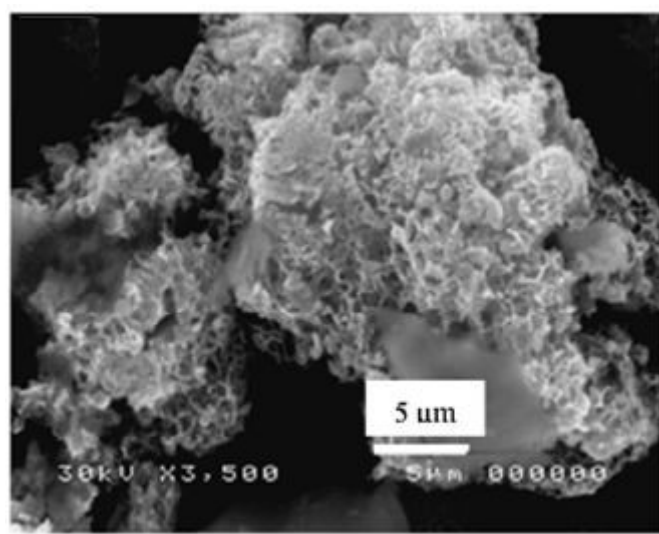


Figure 4: SEM of NiMo/LDH.

4.3 FTIR analysis

The distinctive bands of the hydrotalcite compounds were depicted in the FTIR chart of the LDH. The stretching of hydroxyl groups and the insertion of H₂O molecules between the layers of LDHs were assigned to cause the wide and broadband at 3400 cm⁻¹ (**Figure 5**). For example, concerning the Zn/Al-CO₃ LDH, the interlayer bridging of H₂O-CO₃²⁻ is the cause of the shoulder at 3050 cm⁻¹. The H₂O bending deformation is represented by the band at 1630 cm⁻¹. The asymmetric stretching of CO₃²⁻ groups is identified by the strong bands about



1370–1380 cm^{-1} . For Al-O groups, Zn/Al-OH translation, and Al-OH de-formation, respectively, the bands at 460, 550, and 790 cm^{-1} may be supported ²⁷.

Article Online
DOI: 10.1039/D4TA00272E

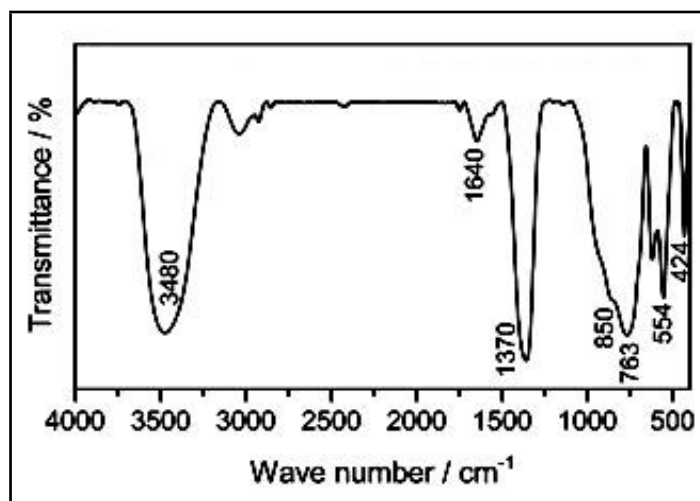


Figure 5: The FTIR spectra of ZnMgAl-LDHs (Zn/Mg = 0.125).

4.4 X-ray photoelectron spectroscopy (XPS)

One important technique for determining the chemical composition, evaluating the oxidation states, and analyzing the electronic structure of layered double hydroxide surfaces is XPS ²⁸ (Figure 6).

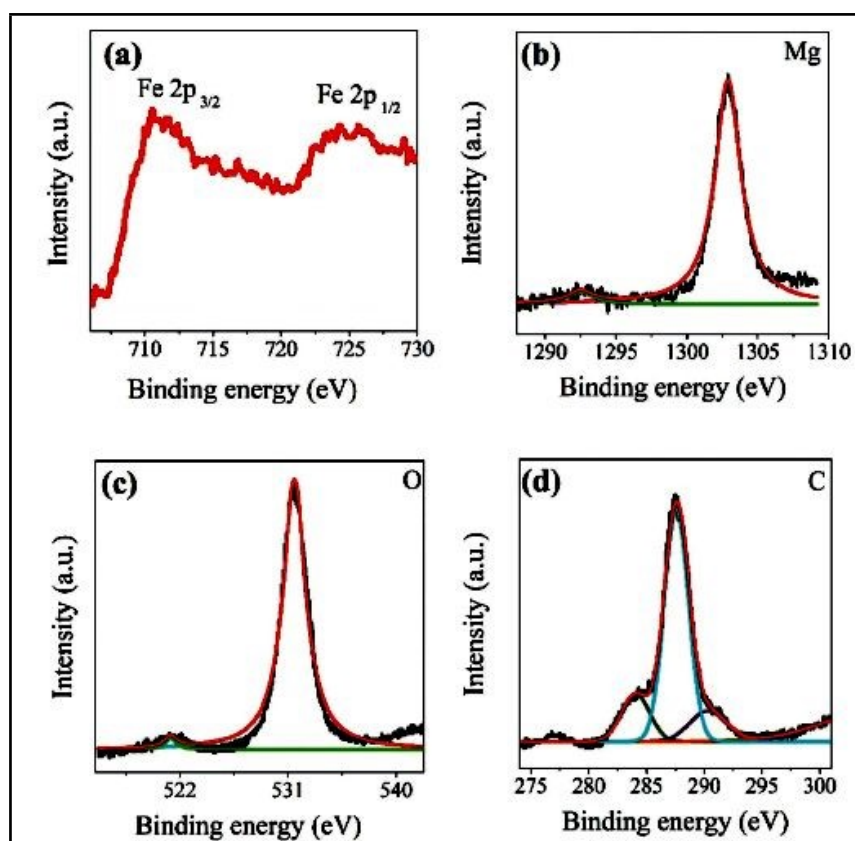


Figure 6: (a) Fe 2p; (b) Mg 1 s; (c) O 1 s; (d) C 1 s orbital XPS spectra for the FeMg/LDH.



4.5 DTA-TGA

View Article Online
DOI: 10.1039/D4YA00272E

DTA-TGA investigations examine weight changes under the influence of temperature. TGA calculates the mass variation of the compounds under various gas or atmospheric conditions, both during heating and cooling. One well-known form of LDH is the TGA of the Zn-Al LDH shows that when the temperature rises, it also determines the loss of interlayer or adsorbed water content as well as the intercalated CO_3^{3-} , NO_3^- -groups, and SO_4^{2-} . According to Wang and co-authors' thermogravimetric investigation of Zn-Al LDH (**Figure 7**), the loss of interlayer water content at the 50–250 °C range resulted in a loss of weight of around 10–14%²⁹. The thermogram for Zn-Al- CO_3 revealed two phases at 150 °C and 250 °C, accompanied by a 21% loss. The dehydration of adsorbed and interlayer water caused the first inflection (at 150 °C), whilst the loss of CO_3^{3-} groups within the LDH interlayers caused the second inflection. Four thermogram phases have emerged for Zn-Al- NO_3 LDH at 150, 250, 350, and 450 °C. The loss of interlayer and surface water molecules caused the first two steps. The dehydroxylation of Zn-Al LDH and the breakdown of the interlayer nitrate anions were responsible for the second two phases, which occurred at 350 °C and 460 °C and resulted in an overall loss of 21.5%.

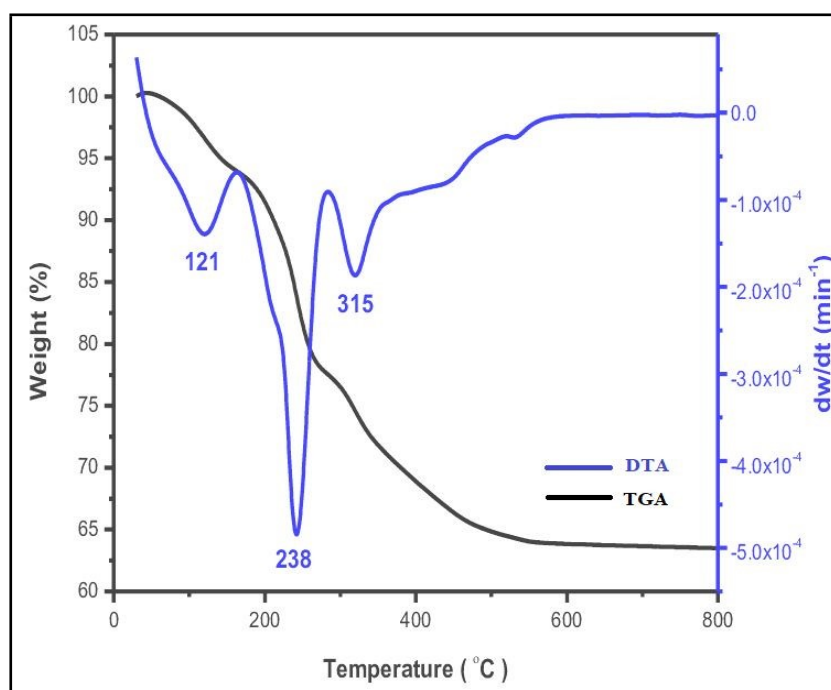


Figure 7: Zn-Al LDH's typical thermogram profile (blue line: DTA scaled on right vertical axis, black line: TGA scaled on left vertical axis).

Advanced methods were reported for the characterization of different LDHs. Raman analysis is considered a diagnostic tool for LDHs, it is widely employed to identify the presence of foreign anions in the interlayer among the brucite-like sheets. Consequently, this technique is always used in combination with others³⁰. Yang et al. studied the adsorption mechanisms of



Cr(VI) by LDH intercalated with EDTA through a multi-approaches analysis which involved XRD, FTIR, X-ray photoelectron spectroscopy (XPS), and zeta potential analysis ³¹.

The Raman spectrum of the LDH sample (**Figure 8**) showed the presence of Fe²⁺ and Fe³⁺ ions in its structure. A sharp band at 1506 cm⁻¹ strongly indicated the presence of Fe³⁺ ions ³², and the band at about 1927 cm⁻¹ corresponded to species of Fe²⁺ ³³, which suggested the co-existence of both Fe²⁺ and Fe³⁺ species in the sample. The presence of Fe²⁺ ions was due to the reduction of Fe³⁺ to Fe²⁺ during the intercalations. The partial reduction of Fe³⁺ to Fe²⁺ might be associated with the hydrogen bonding between the interlayer water molecules or hydroxyl groups of the LDH sheets and the Fe³⁺ cations. As assigned above, the bands at 1061 cm⁻¹ and 1262 cm⁻¹ were assigned to the vibrations of the carbonate species (CO₃)²⁻ ³⁴.

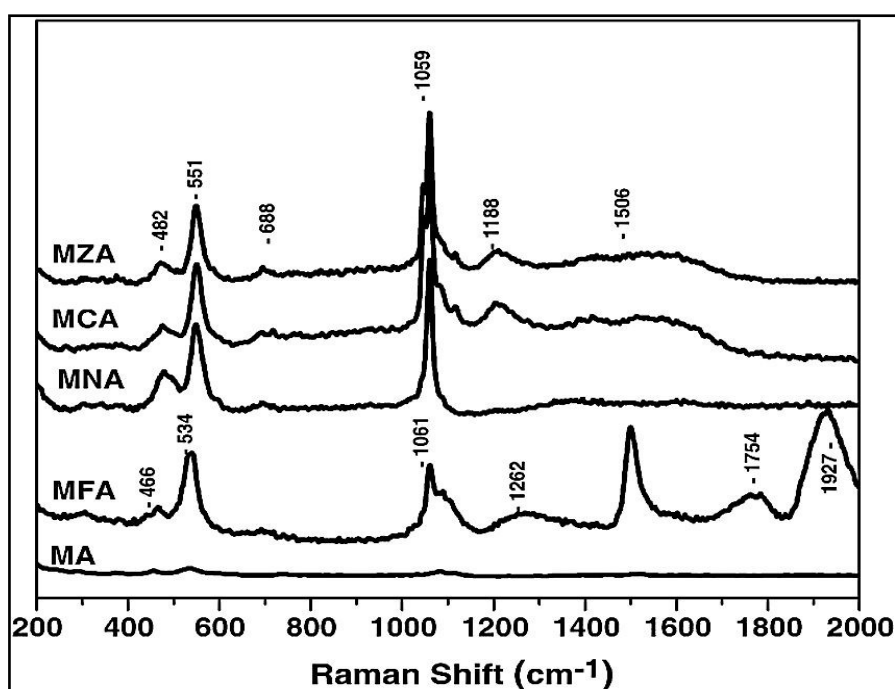
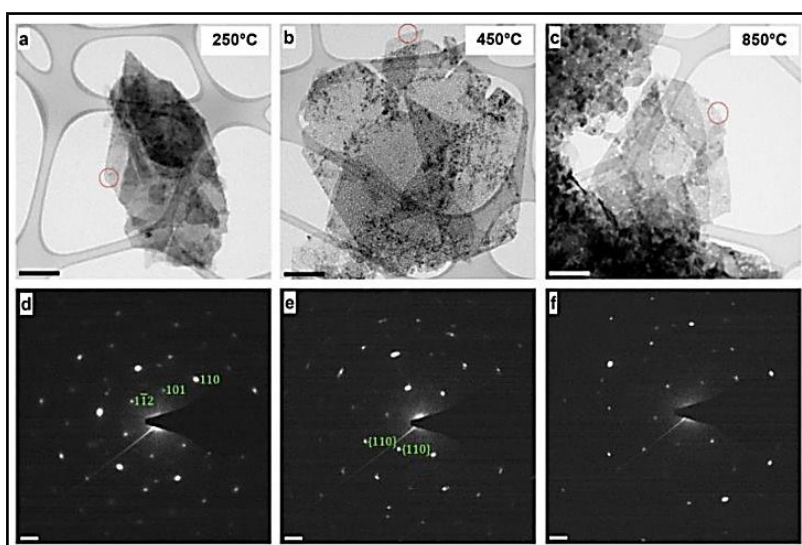


Figure 8: Raman spectra of the different LDH samples.

A commonly employed way to characterize nanosized materials is to couple transmission electron microscopy (TEM) and selected area electron diffraction (SAED) analysis. Hobbs et al. ³⁵ applied in-situ TEM to comprehensively characterize LDH nanomaterials. The combined approach of TEM and SAED allowed both a morphological and crystallographic understanding of the LDHs (**Figure 9**).





View Article Online
DOI: 10.1039/D4YA00272E

Figure 9: Transmission electron microscopy (TEM) images and associated selected area electron diffraction (SAED) patterns of the Ni/Fe LDH.

A novel approach was applied for the characterization of LDHs was reported by Dionigi et al.³⁶ which combined operando X-ray scattering and absorption spectroscopies to elucidate the active phase and the mechanism for the oxygen evolution reaction (OER) application. Despite previous reports on the ex-situ crystal structure of the as-synthesized precursors of M/Fe LDH catalysts and in situ local structure based on XAS measurements; little was previously known about the long-range crystal structures of the catalytically active phase during application conditions. Combining electrochemical measurements and operando wide-angle X-ray scattering (WAXS), XAS data with computational simulations that were specifically for the strongly correlated Fe, Co, and Ni oxides and (oxy)hydroxides, assisted in unraveling the crystal structures and electro-catalytic OER mechanisms of the active phases of Ni/Fe and Co/Fe LDH catalysts.

5. Promising LDH uses

The unique nanostructure of layered double hydroxides, the occupancy of multiple metal cation types within their layers, the active -OH groups on their surface, the simplified preparation routes, the non-toxicity, the flexible changing of both cations and anions, the outstanding anion replacement ability, memory retentive, the high efficient to transport the intercalated anion in a sustained mode, the bio-compatibility, the electrochemical activity, the high surface and pore size, the high adsorption capacity and efficacy, make LDH composites a promising category of the nanomaterials. LDH and their intercalated form with various functional precursors, as well as nanocomposites containing superior nanomaterials, primarily carbon nanomaterials, are regarded as effective precursors for essential applications because of their remarkable properties. Applications for LDHs and their modified forms include water



splitting, wastewater treatment, oil transesterification for the manufacture of biofuel, and catalysis. View Article Online
DOI: 10.1039/D4YA00272E

5.1 Biofuel manufacture using transesterification process catalyzed by LDH

Transesterification and pyrolysis are the two primary procedures used to produce biofuel from oils and fats^{37,38}. Triglycerides and short-chain alcohols combine during the transesterification process to produce the fatty acid (FA) monoester^{39–41}. Pyrolysis is the process of heating triglycerides without the use of catalysts (thermal cracking) or with the catalysts (catalytic cracking)^{42–46}.

Because of the presence of metal oxides and the electropositivity of the cations present in their composition, LDH acquired active sites that are effective during the transesterification reaction, and that can be classified as Lewis-base catalysts⁴⁷. The layered double hydroxides' chemical activity was enhanced by the various metal cations that were present in their structures. It makes sense that the temperature at which the cations are calcined, as well as their valence and ionization states, affect the catalytic activity⁴⁸. Numerous reports have discussed the function of mixed oxides' basic sites and other physical-chemical characteristics in the transesterification process.

By using the co-precipitation approach, LDH with the formula $[\text{Mg}_{(1-x)}\text{Al}_x(\text{OH})_2]^{x+}(\text{CO}_3)_{x/n}^{2-}$ ($x=0.25-0.55$) was created⁴⁹. To create the appropriate biodiesel, the obtained materials were added through the transesterification of glyceryl tributyrate in the presence of methyl alcohol. As the magnesium concentration rose, the conversion rate rose. The comparative research conducted by Boey et al., between thermally treated crab shells and laboratory-prepared CaO, revealed no discernible differences in the CaO sources used in the transesterification reaction of *palm oil* to biodiesel⁵⁰. Li-Al, Mg-Al, and Mg-Fe were the three produced calcined LDH that were employed to create the appropriate biodiesels by methanol utilizing two triglycerides, namely: glyceryl tributyrate and *soybean oil*⁴⁷. In terms of fatty acid methyl ester yields, Li-Al layered double hydroxide showed the maximum activity when used at 65 °C, but Mg-Fe and Mg-Al LDH showed lower activity. In contrast to the large concentration of weak basic sites on the surfaces of Mg-Al and Mg-Fe LDH, the greater activity of Li-Al LDH was ascribed to the existence of a high concentration of the medium and strong basic sites on its surface. These results were obtained using CO₂-TPD spectroscopy, which offers a clear picture of the different kinds and intensities of active sites on the catalyst surface. The greatest activity for Li-Al was attributed to the noncrystalline nature of lithium aluminate due to the structure breakdown into the equivalent mixed oxide at the calcination temperature of 450–500 °C. Similar findings were reported by Sankaranarayanan et al.,⁵¹ who found that



calcined Ca-Al₂ LDH exhibited great activity in converting non-edible, and edible oils into biodiesels. The high basic characteristics of the catalyst, which were ascertained using Hammett CO₂-TPD elucidation, were credited with the activity of the used Ca-Al₂ LDH .

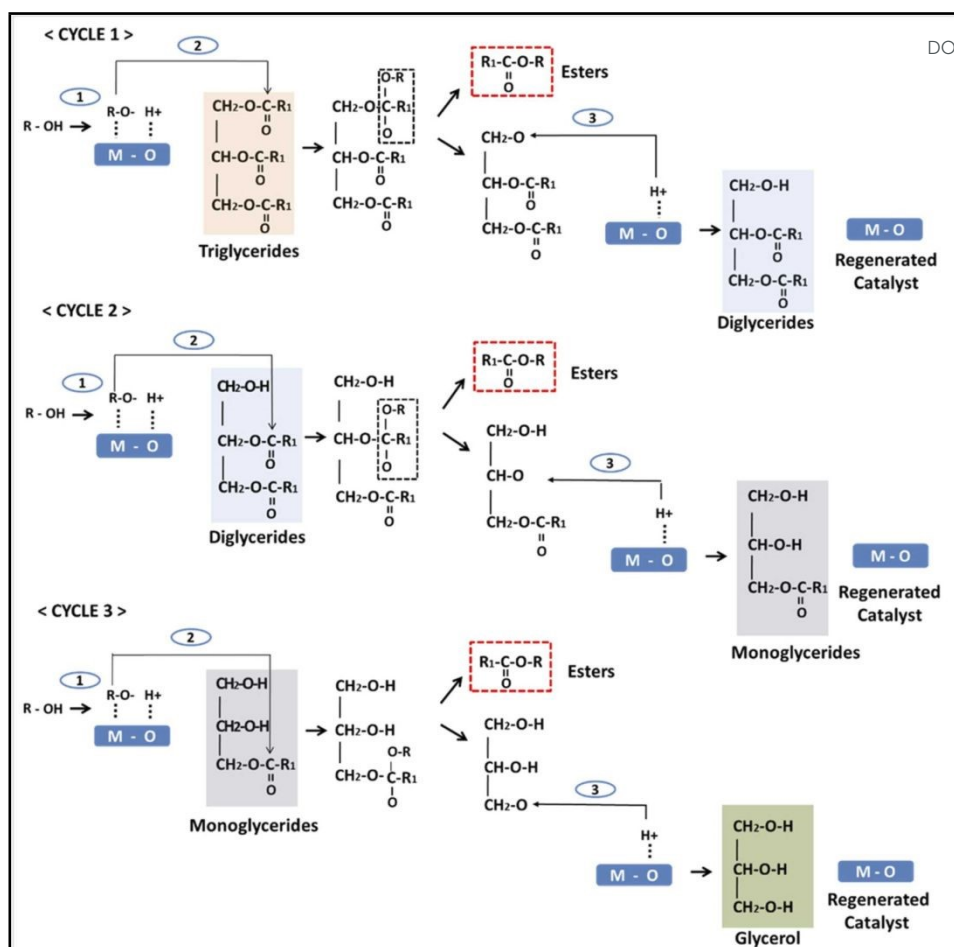
The adsorption of the reactants occurs on positions of the catalysts surfaces known as the active sites, as part of the transesterification reaction process that has been described in many phases ⁵²⁻⁵³. In the transesterification media, the LDH acts as heterogeneous catalysts and is supplied as solids alongside glycerol and biodiesel. One significant benefit of heterogeneous catalysts is their ease of separation and recycling ⁵⁴.

A categorical and motivating transesterification mechanism was proposed and reported ⁵⁵. During this mechanism (*Scheme 1*), the initialization step is initialized due to the basic nature of the LDH catalysts. In the reaction mechanism cycles, cycle 1 presented the abstraction of the protons in the hydroxyl group of the alcohol (methyl alcohol) as the influence of the basic sites of the LDH to obtain the methoxide anions. In cycle 2, the formed methoxide anions attack the carbon formed the carbonyl groups found in the oil molecules to form an intermediate (alkoxycarbonyl) which easily degenerates into fatty acid methyl ester (FAME) and diglyceride molecules. In final stage, the diglyceride anions contained the oxygen attacked the proton linked to the LDH base, which leads to formation of the catalytic sites. Subsequently, series of interactions occurred for the di-glycerides and the mono-glycerides to form the final product of the biodiesel molecules.

The mechanism of catalytic transesterification of waste cooking oil (WCO) using ZnAl/LDH@SiO₂ was reported by Fereidooni et al ⁵⁶, and illustrated in *Figure 10*. As reported, Si atoms are prone to connect to oxygen atoms in triglyceride which highly supports electrophilicity on sites of triglyceride carbonyl, Consequently, the loading of SiO₂ on LDH sheets promotes the oxygen atoms to interact and also accelerates the attack of the triglyceride carbonyl group by the methoxides molecules and increases the catalytic activity of LDH.

View Article Online
DOI: 10.1039/D4YA00272E





Scheme 1: Mechanism of transesterification.

Figure 10: Suggested mechanism of transesterification process using ZnAl/LDH-SiO₂ composite.

5.1.1 Structural factors affect LDH activity in the biofuel manufacturing process

View Article Online

DOI: 10.1039/D4YA00272E

The preparation conditions and methods of layered double hydroxides have a significant impact on the hydroxides' surface characteristics. The LDH calcination process, the medium's acidity or basicity, the reaction temperature, the concentration of the reacted metal ions, and the reaction duration are all considered preparatory conditions. Co-precipitation, hydrothermal, sol-gel, and other methods are among the preparation techniques⁵⁷.

5.1.1.a LDH calcination procedure

The components of layered double hydroxides are reorganized significantly during the heat treatment (calcination process)²³. The catalytic activities of layered double hydroxides, such as the activity of the basic strength reactive sites and increased reactive surface area, are supported by this procedure.

5.1.1.b The basicity of LDHs and basic locations

The occurrence of deformation in the catalyst's crystalline structure explains the creation of the basic site mechanism. Metal oxides are incorporated into the distorted crystals as a result of calcination, offsetting the positive charges that are produced. The fundamental active sites in the distorted system are produced by the presence of O²⁻ anion. When the created basic sites are found in the function groups OH⁻, Mg-O, and O²⁻, they may be categorized as weak, medium, and strong sites³.

5.1.1.c Metal ion doping in LDHs

It has been observed that the chemical structures of various metals may modify the surface basicity of layered double hydroxides, hence changing their activity. Fe³⁺, Cu²⁺, and Zr²⁺ are the most reactivating metal ions. The layered double hydroxides doped by Cr³⁺, Fe³⁺, Cu²⁺, Mn²⁺, Co²⁺, Ni²⁺, and Zn²⁺ improved their catalytic activity throughout the transesterification process, according to the CO₂-TDP analysis⁵⁸.

5.2 Catalysis performance

Layered double hydroxides' adaptable structure and adjustable basic characteristics explain their catalytic function and match their intended use⁵⁹. As heterogenous base catalysts, LDHs have great selectivity and potential for a wide range of catalytic processes, mostly organic transformations (*Scheme 2*), such as condensation, redox reactions, alkylation, hydroxylation, isomerization, hydro-formylation, and transesterification. Additionally, the mixed oxides that resulted from the LDHs' thermal treatment (calcination) show various organic reactions and worthwhile catalytic activity⁶⁰.

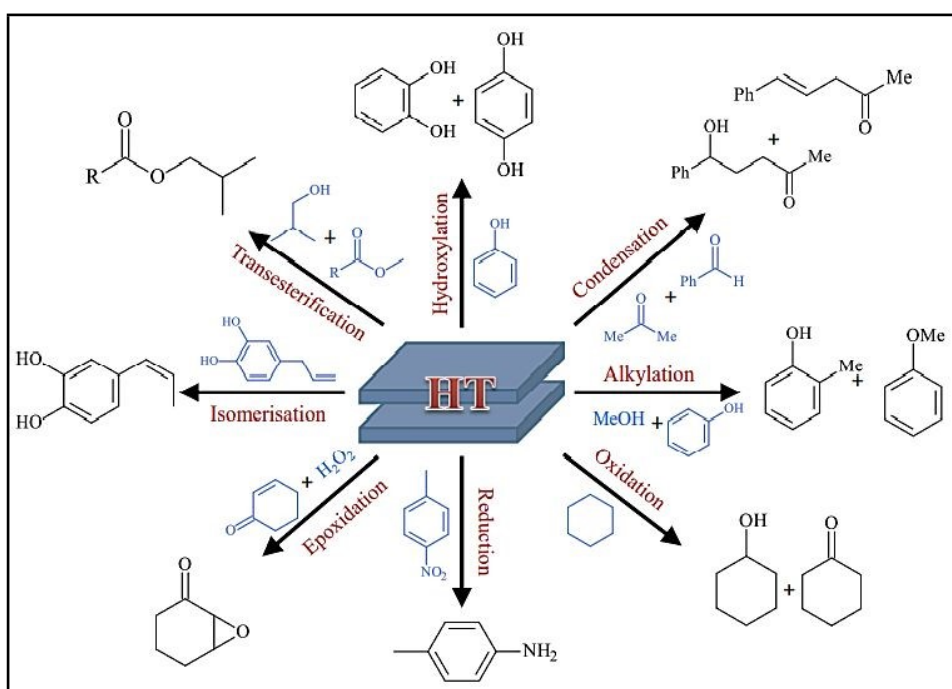
Yan et al.,^{61–63} presented a concise review representing detailed information about the different mechanisms that occurred during the application of LDHs composites in oxygen



evolution reaction, hydrogen evolution reaction, urea oxidation reaction, nitrogen reduction reaction, and biomass derivatives oxidation.

Lignin is one of the main constituents of lignocellulosic biomass, which could provide an abundant source of aromatic compounds. The efficient utilization of lignin is believed to be a promising strategy to address the current energy crisis. However, the complex structure and rich oxygen-containing groups of lignin hinder its valorization into value-added chemicals⁶⁴. Hydrodeoxygenation (HDO) of biomass-derived derivatives has been widely considered an efficient and feasible strategy to remove excess oxygen content in lignin. LDHs are promising to be suitable precursors to construct bifunctional catalysts with both small-sized metal centers and acid sites for conversion reactions. Kai et al.,⁶⁵ reported the conversion of vanillin (as a simulant for biomass comparable to lignin).

Both thermally modified and unmodified LDHs have found extensive application as stable, recyclable heterogeneous catalysts or catalyst supports for a range of processes that benefit from the easy exchangeability of intercalated anions and the flexible tuneability and uniform distribution of metal cations in the LDH layers. Because of the availability of the hydroxyl groups, LDHs are attractive heterogeneous solid base catalysts for a variety of chemical reactions. LDHs have been converted to mixed metal oxides with multiple Lewis base sites and increased surface area during heating between 450 and 500 °C, yielding good catalytic efficiency. In the absence of CO₂, the mixed metal oxide may be rehydrated to form LDH with an OH-intercalated anion.



Scheme 2: Schematic illustration of organic reactions catalyzed by LDH.



5.2.1 LDH intercalation

View Article Online
DOI: 10.1039/D4YA00272E

The addition of a third cation to the binary LDH composites to create the modified forms has up surging influence on their catalytic efficiencies during catalyzing the organic reactions. The type of cations used in the makeup of the intercalated anion determines the catalytic activity of layered double hydroxides. Based on these anions' size and chemical makeup, or nuclearity, the intercalated anions vary from one to another.

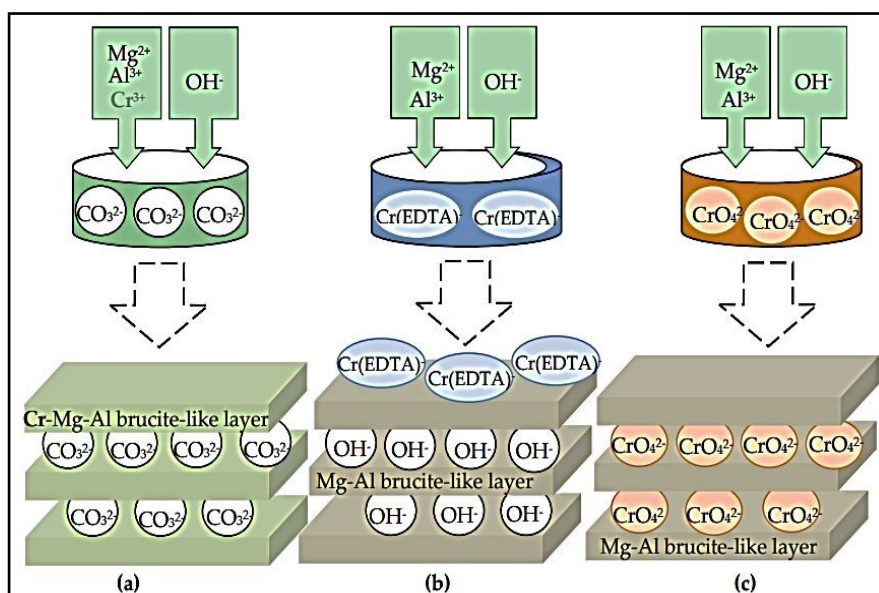
5.2.1.a Intercalated LDH with small-nuclear polyoxometalate anions

Low-nuclear polyoxometalates (POM) are present in LDH systems and are primarily intercalated by chromate, dichromate, and chromium anions such as Cr-(EDTA), [Cr-(SO₃-salen)]²⁻. These LDH variants exhibited good catalytic activity, particularly in alcohol oxidation and alkoxylation. The intercalation of chromates in LDH is worthy of high consideration due to its applications in the remediation of wastewater and also has valuable applications in the catalysis of numerous reactions with important products. CrO₄²⁻ and Cr₂O₇²⁻ anions are deceptive anionic contaminants found in wastewater ⁶⁶.

Co-precipitation, anion exchange, and reconstruction of the mixed oxide procedures were reported as effective methods for the synthesis of LDH containing M²⁺/M⁺³ cations interpolated with chromate in the brucite-like layers ⁶⁷⁻⁷⁰. **Scheme 3** shows the synthetic strategies used to prepare LDH precursors of chromium catalysts. These strategies include (i) co-precipitation of metal cations with carbonate counter-ion under basic conditions; (ii) co-precipitation of Mg(II) and Al(III) with EDTA chelate of Cr(III) form a chelate of 1:1 stoichiometry with (EDTA), as EDTA is thermodynamically stable compared to Mg(II) or Al(III) ⁷¹; and (iii) co-precipitation of Mg(II) and Al(III) with CrO₄²⁻ anions existing at the slightly excess concentration required for stoichiometry in the medium. Good catalytic activity was shown by the LDH-intercalated sulphonate-salen-chromium (III) during the selective oxidation of glycerin in the existence of 3% H₂O₂ to create dihydroxyacetone. This was explained by the sulphonate-salen-chromium (III) and the weak base LDH having a balancing effect on each other. A series of POM/LDH nanocomposites were made by Malherbe et al., using Cr²⁺ and Cu²⁺ cations to create layered double hydroxides, with CrO₄²⁻ or Cr₂O₇²⁻ anions intercalated among the LDH layers. The compounds have been evaluated in the catalytic synthesis of glycol ethers in the catalyzed ethoxylation process of butyl alcohol with ethylene oxide ⁷².

The intercalated LDH with various chromium-based anions, such as chromate, dichromate, Cr-(EDTA)⁻, and [Cr-(SO₃-salen)]²⁻, are excellent catalysts for a variety of catalytic reactions due to their low-cost of precursors, easy synthesis, and superior stability.





Scheme 3: Synthetic methods for producing chromium catalyst LDH precursors.

5.2.1.b LDH intercalated with medium-nuclear polyoxometalate anions

LDH composites intercalated with medium-nuclear polyoxometalates may accept anions based on vanadium or molybdenum. Layered double hydroxides of molybdate and vanadate (Mo-LDH, V-LDH) have effective catalytic activity in oxidation and epoxidation processes.

5.2.1.b.1 Vanadates

The most documented methods for creating the layered double hydroxides intercalated with vanadate anions include co-precipitation, anion exchange, reformation, and hydrothermal methods which provide hosting the vanadate anions between the M^{2+}/M^{3+} cations in the brucite-like layers. Depending on the building cations and the acidity or basicity of the solution, vanadium anions may be interlayered in the layered double hydroxides and can be also added as a cation V(III) in the LDH of the brucite-type layers.

After pre-swelling with terephthalate, Villa et al. described a straightforward method of preparing decavanadate-intercalated LDH containing Mg^{2+} and Al^{3+} cations. This was achieved by a direct ion exchange of nitrate precursor with a mildly acidic $NaVO_3$ medium. It was shown by the Raman, IR, and XRD patterns that there is decavanadate ($[V_{10}O_{28}]^{6-}$) anions in the interlayer area. Decavanadate-intercalated LDH that has been synthesized is classified as an allylic and homo-allylic alcohol-specific epoxidation catalyst⁷³. Maciucă et al. produced LDHs intercalated with decavanadate and pervanadate anions immediately in a procedure identical to this one. Through the catalytic oxidation process of tetrahydrothiophene to sulfolane in the presence of hydrogen peroxide, the produced LDHs' oxidative catalytic activity was evaluated⁷⁴.



5.2.1.b.2 Molybdate

View Article Online
DOI: 10.1039/D4YA00272E

Predominant molybdate anions are $[\text{MoO}_4]^{2-}$, $[\text{HMoO}_4]^-$, $[\text{Mo}_6\text{O}_{19}]^{2-}$, $[\text{Mo}_7\text{O}_{24}]^{6-}$, $[\text{HMo}_7\text{O}_{24}]^{5-}$, $[\text{H}_2\text{Mo}_7\text{O}_{24}]^{4-}$, and $[\text{Mo}_8\text{O}_{26}]^{2-}$. The intercalation of molybdenum-based anions in the structure of layered double hydroxides is dependent upon the pH of the medium and the concentration of Mo(VI) cations. Due to the formation of heptamolybdate $[\text{Mo}_7\text{O}_{24}]^{6-}$ ions, which may be stable at low pH levels and increase the spacing between the brucite-type sheets, the intercalation of molybdates has been inhibited in the interlayer space of layered double hydroxides⁷⁵. Within the context of the MgAl-LDH composite, the anionic exchange approach is generally applicable during molybdate assimilation. A novel approach based on the traditional ionic exchange method was published by Soled et al, It involves the synthesis of an anion-pillared organic precursor, which is then substituted in acidic environments by an appropriate polyoxometalate anion⁷⁶.

5.2.1.c Intercalated LDH with high-nuclear polyoxometalate anions

The majority of LDH systems containing high-nuclear polyoxometalates are intercalated by tungsten anions. The catalytic activity of layer double hydroxide intercalated with tungsten anions was shown to be effective in the oxidation of organosulfur compounds such as benzo- and dibenzothiophene, as well as the epoxidation of alcohols. Polyoxotungstates are present in many forms and sizes, possess set dimensions, and have a wide range of applications⁷⁷. The temperature, the length of time it takes for LDH and polyoxometalates to react, and the medium's pH all have a significant impact on how the intercalated LDHs are prepared inside tungstate-based anions⁷⁸. The interlayers of the layered double hydroxides are intercalated by polyoxotungstate structures and have a variety of forms, including Keggin, Dawson, and Finke types.

Methoxybromination of aliphatic olefins produced moderate chemoselectivity, but methoxybromination of aromatic and aliphatic olefins produced strong regioselectivity and stereoselectivity⁷⁹. Utilizing Mg-Al-Cl-LDH and Ni-Al-Cl-LDH exchanged with tungstate in mild oxidative bromination reaction was reported⁸⁰. Organotungstic compounds with modified Mg-Al-hydrotalcite intercalated acted as a catalyst for the epoxidation of cyclohexene. Anionic exchange and complexation with added phosphonic acid in the sheets were used to execute the modified Mg-Al-LDH⁸¹. Using nitrate LDH precursors as an initial material, polyoxometalates $[\text{H}_2\text{W}_{12}\text{O}_{40}]^{6-}$ and $[\text{W}_4\text{Nb}_2\text{O}_{19}]^{4-}$ have been synthesized and intercalated in brucite-like layers of Mg-Al- and Zn-Al-LDHs by anion exchange technique. Using hydrogen peroxide, the cyclooctene epoxidation process was catalyzed by the modified



LDHs⁸². LDH composite of Mg-Al-SiW₁₂O₄₀, Mg-Al-PW₁₂O₄₀, and LDH virgin Mg-Al-LDH enhanced the photocatalytic degradation of malachite green (MG)⁸³. (View Article Online
DOI: 10.1039/D4YA00272E

.52.2. Layered double hydroxides reinforced with materials derived from carbon

Assembling hollow flower-like LDH and N-, S-doped graphene acting as support for Pd-NPs gave hollow inner and mesoporous hierarchically flower composites. LDH/nanocarbon catalysts have been given significant consideration for their significance in various reactions such as Michael addition⁸⁴, Knoevenagel reaction⁸⁵, Ullman reaction⁸⁶, Sonogashira reaction, Heck reaction, and chalcone synthesis⁸⁷. By intercalating LDH with reduced graphene oxide (rGO)⁸⁸, as well as multi-wall carbon nanotubes (MWCNT)⁸⁹, sandwich-like structures were produced. One of the main characteristics of LDH/carbon composites is thought to be interfacial electron transfer⁹⁰, which is aided by the carbon components' high electronic mobility. Due to the interaction with the less conductive LDHs, this results in charge redistribution. Enhancing electron transport is possible using carbon dots-based LDH/nanocarbon^{91,92}. During glucose electro-oxidation, the Ni-Al LDH/CNTs nanocomposite displays electro-catalytic activity instead of the Ni-Al LDH electrode or the CNTs electrode⁹³. This was ascribed to carbon nanotubes' (CNT) capacity to move extra electrons between Ni ions and electrodes, as well as, to encourage reactant diffusion across the given porous complex framework⁹⁴. The high strength and reusability of LDH/CNT catalysts were important characteristics that characterized the LDH intercalated by carbon nanotubes during application. It was constructed using LDHs and had a high mechanical strength of CNT in its purest form. Furthermore, effective regeneration of the catalytic active sites and high stability against leaching is achieved by the strong metal-CNT contact.

5.3 Water splitting

Hydrogen as a sustainable energy source, is an alternative to conventional petroleum fuels for mitigating soil contamination and the development of warming gasses⁹⁵. Generation of hydrogen from water splitting reaction of water using photocatalytic reactions is a promising source of energy due to its environmental and clean resource. The water splitting reaction under influence of irradiation can be occurred when the energy of the conduction band is more negative than the reduction potential of the hydrogen protons to hydrogen atoms and the valence band is more positive than the potential of oxidation of oxygen atoms to oxygen anion. The photocatalytic water splitting reaction is occurred through three stages: the photocatalyst absorbs photon energy higher than the bandgap energy of the water, which generates electron rich (electron)/ electron deficiency (holes), follows by migration to the surface of the photocatalysts, and finally the occurrence of the reduction/oxidation reactions

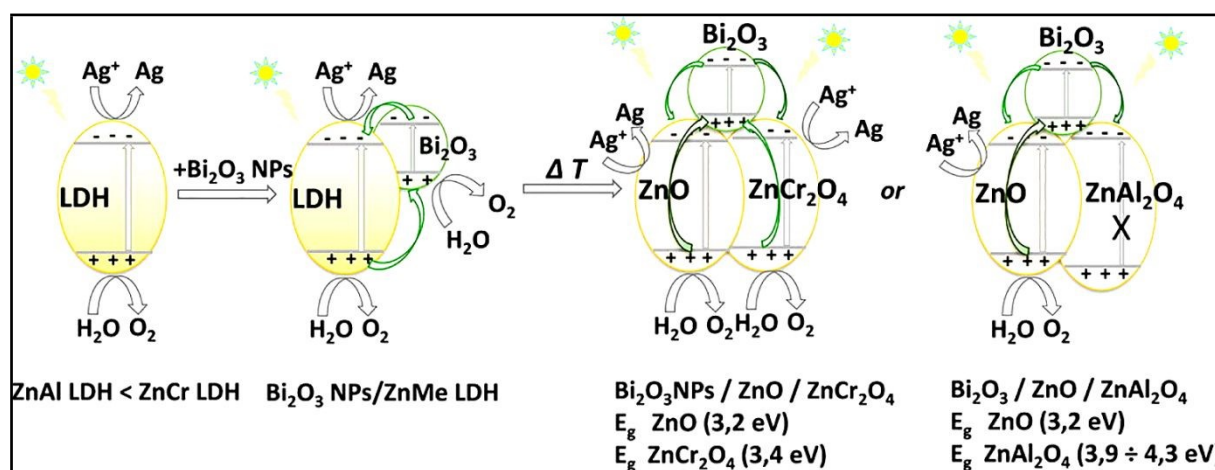


between the formed charges and the water molecules to generate the hydrogen and the oxygen

96.

For the LDH composites, the formed surface charges after generation are transferred to the active sites within finite short time ranged between nano- to microseconds⁹⁷. The initial two steps are depending on the structure and electronic configurations of the LDH photo-catalysts. The high crystalline LHD has a positive influence on the photocatalytic activity, and the density of the morphological defects acting as recombination centers between the generated carriers which decrease with the increase of the crystallinity. The specific photocatalytic water splitting mechanism in case of LDH composites is occurred due to the excitation of electrons from the ground state into the excited state followed by the separation of the formed charges as a result of the formation of positive holes and negative centers due to the excitation process, the excitation is occurred throughout $d-d$ electronic transitions, metal-to-metal and ligand-to-metal charge transfer⁹⁸.

The photocatalytic mechanism of $\text{Bi}_2\text{O}_3/\text{ZnO}/\text{ZnMe}_2\text{O}_4$ LDH was extensively reported in the work of Boumeriame, et al⁹⁹. Bi_2O_3 NPs LDH shows the typical water splitting mechanism (O_2 generated in the VB of both moieties and the Ag particles being reduced on the CB), **Scheme 4**. After the calcination, the photogenerated holes of Bi_2O_3 decrease the overall recombination rate by balancing the electrons from the CB of the ZnO and ZnMe_2O_4 matrices; in the case of ZnAl_2O_4 the band structure does not allow for water oxidation and, thus, $\text{Bi}_2\text{O}_3/\text{ZnO}/\text{ZnCr}_2\text{O}_4$ presents a higher OER rate.



Scheme 4: Proposed mechanism for O_2 -generation under solar-light irradiation over Bi_2O_3 NPs/ZnMe-LDH and Bi_2O_3 /ZnO/ZnMe₂O₄.

5.4 Formation defect

Deformation of LDH composites is performed mainly by doping foreign metal cations into their crystalline structures. Doping with foreign metal cation to form single phase ternary



metal compounds could boost the HER and OER catalytic performance, such as Fe-doped CoP, Fe-doped Ni₂P, Co-doped Ni₂P, Co-doped FeS₂, V-doped NiFe LDH, and some other metal-doping in metal compounds¹⁰⁰. Based on the theoretical mechanism theories, introducing of foreign cations can change the initial electronic structures according to two different metal 3d-orbitals and can also improve the absorption Gibbs free energy toward intermediates, which improves the electro-catalytic activities.

The presence of electronic vacancies in the *d*-metal based compounds, such as oxygen, sulfur, and selenium, can modify their electronic configuration and enhance the electrocatalytic activities¹⁰¹. In case of metal oxide catalysts, generating oxygen vacancies enhances the catalytic activity because the electrons tend to collect nearby the valence band maximum of metal oxides with oxygen vacancies to form electron rich centers. The electron-rich centers acted as catalytic active sites which stabilize the reactants and reaction intermediates. That leads to lower the activation energy barrier and consequently catalyze the electrochemical reactions.

5.5 Transfer of charges

Since modified layered double hydroxides (LDHs) have remarkable two-dimensional and compositionally variable structures, they have been investigated as catalysts for optical and electrochemical processes¹⁰². LDHs provide space and position separation of redox-reaction sites for efficient production of hydrogen and oxygen through the water-splitting process. Because of their large adsorption capability and tunable band gap, they are suitable for the ionic exchange process (cation-anion exchange)¹⁰³. Additionally, the lamellar structures of LDH allowed for a variety of cation and anion types as well as crystalline sizes, forms, and morphologies. These characteristics have a significant impact on the efficiency of charge transfer and separation, which in turn raises concerns about the photo-catalytic energy process's efficiency¹⁰⁴. The most recent changes to LDH were made to its size, shape, electrical characteristics, and chemical structure. By selecting novel carbon supports, such as carbon quantum dots¹⁰⁵, graphene oxide¹⁰⁶, graphdiyne¹⁰⁷, and graphitic carbon nitrides¹⁰⁸, the electrical characteristics and charge separation capabilities were altered. These substrates possess the capacity to support layered double hydroxides' photo- and electro-catalytic properties.

In electro-catalytic processes, LDH materials having transition metal cations, particularly Ni and Co have found widespread use. In LDH hosts, the intercalation of POMs and simple metal oxy-anions may result in photo-catalytic activity. The distinct lamellar structure and abundant active sites of LDHs containing various transition metals (e.g., Co, Ni, Fe, etc.)



make them excellent electro-catalysts. A method for transforming inexpensive Fe substrates into ultra-stable electrodes for the oxygen evolution reaction was enhanced by Yipu et al¹⁰⁹, This method was achieved by using aqueous solutions containing oxygen and Ni²⁺ at room temperature to corrode Fe substrates. Instead of producing rust, this method produced nano-sheets of Fe-containing LDH on iron. According to Yan et al., there was a significant improvement in the electrodeposition-support of graphene layers encircled by NO³⁻ ions. The generated cerium dioxide in the nano-crystalline and amorphous forms of Ni(OH)₂ for the electro-catalytic oxygen evolution process showed a reduced over-potential value of 177 mV at 10 mA.cm⁻² current, with good durability reaching 300 hours at 1000 mA.cm⁻² ¹¹⁰. Direct electro-deposition of nickel foam produced amorphous mesoporous Ni/Fe nano-sheets, which were then used as O₂-electrodes for the O₂ evolution process during the water-splitting reaction ¹¹¹. To deliver 500 mA.cm⁻² and 1000 mA.cm⁻² current densities at 240 mV and 270 mV potentials, respectively, the electrode demonstrated good efficacy through the water splitting reaction in an aquatic medium with 200 mV potential ¹¹¹.

LDHs improved by various transition metal ions including Fe, Co, Ni, Zn, and Mn were extensively studied. A series of catalysts, including metal oxides ¹¹², metal hydroxides ¹¹³, metal selenides ¹¹⁴, metal sulfides ¹¹⁵, metal carbides ¹¹⁶, and metal phosphides ¹¹⁷, were established for the oxygen evolution reaction in an alkaline aquatic environment. Yang et al. ¹¹⁸ created LDHs modified by cobalt, and nickel and intercalated their structures with CoNiSe₂ to catalyze H₂O-chemisorption and produce reactive hydrogen-containing intermediates, which effectively split water. As a result, a layered double hydroxide hybrid structure was created by electro-depositing amorphous NiFe hydroxides on the surface of NiFeP ¹¹⁹. The resulting catalysts exhibit strong electrical interactions that may be used to increase the water-splitting process by lowering the adsorption energy of water. By combining metal phosphides with NiFe-layered double hydroxides, one may concurrently perform a bi-functional oxygen evolution process of H₂ and O₂ making up for the shortcomings in each catalyst ^{120,121}.

5.6 Treatment of wastewater

The rapid advancement of industrial and agricultural growth is to blame for the massive and varied releases of pollutants into water bodies ^{122,123}. As a result of these advancements, many contaminants such as metals, dyes, oxygenated anions, and emerging organic compounds contaminate rivers and undersea environments. Wastewater is treated utilizing LDHs in several ways (*Figure 11*).



Dyes are used in the food, pharmaceutical, paper, and textile industries. Roughly 10% to 15% of dyes are released into water resources by the textile industry. Because the dyes harm photosynthesis and, in turn, the concentration of oxygen in aquatic systems, their low concentrations pose harm to the environment. Moreover, hazardous and cancer-causing intermediates are produced by the degradation processes of many dyes¹²⁴. Several industrial anionic and cationic dyes are effectively eliminated by LDHs¹²⁵. When it comes to eliminating cationic and anionic dyes, respectively, LDHs and activated carbon behave in the same way¹²⁶.

The excellent remediation effectiveness and adsorption capacity of several LDHs for the removal of cationic dyes have been widely documented¹²⁵. Using the co-precipitation technique, two distinct layered double hydroxides (Mg-Al LDHs) were produced utilizing dodecyl sulfate (Mg-Al-DS) and carbonate (Mg-Al-CO₃), and their ability to uptake methyl orange from wastewater was evaluated. The maximum capacities for Mg-Al-DS and Mg-Al-CO₃ were 185.1 mg/g and 97.5 mg/g, respectively. The mechanisms of the adsorption reaction were proposed as anions exchange of Mg-Al-CO₃ for methyl orange anions dye and; the association of dye anions to positive charges of LDHs¹²⁷. The pH of the medium does not affect the efficiency of Mg-Al-DS LDH, but the efficiency of Mg-Al-CO₃ LDH is increased by an acidic to neutral medium.

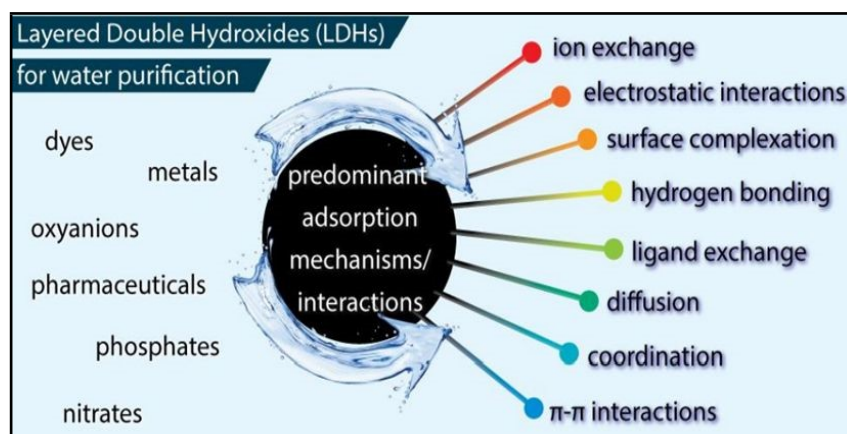


Figure 11: LDH-based techniques used for wastewater cleaning.

The co-precipitation method was utilized to create carbonate anions LDH (Mg-Co-Al-CO₃ LDH), which was then used to remove RB19 dye from wastewater¹²⁸. The produced LDH was proposed to play three roles: chemical bonding, physical adsorption, and electrostatic attraction. Using the precipitation approach, Ahmed et al. organized Mg-Fe-LDH nanoparticles and used them to adsorb Congo red dye from an aquatic medium. Physical and chemical interactions were the produced LDH's adsorption roles¹²⁵.



Large volumes of heavy metals, including cadmium, lead, mercury, copper, nickel, chromium, and arsenic, are discharged into the environment by industrial operations, particularly those related to batteries, electroplating, and mining. Transition metal ions are very poisonous and accumulate in nature^{129–131}. The Satoshi Fujji group¹³² was the first to describe using LDHs as adsorbents for Pb^{2+} , Cu^{2+} , and Zn^{2+} . The remediation of metal ions by layer double hydroxide has been described via several processes or interactions, including surface complexation, isomorphous substitution, surface precipitation, electrostatic interaction, and chelation¹³³. Ca-Fe double hydroxides LDHs were created by modifying them with 3-aminopropyl triethoxysilane. Their nanocomposites were then assembled in 5% and 10% mixing ratios with polyaniline¹³⁴. When Pb^{2+} ions were being adsorbed from their aqueous solution, the produced composites were applied. The adsorption capacity of the LDH composite containing 10% polyaniline was 110 mg/g, while the one containing 5% polyaniline showed a capacity of 56 mg/g.

Using a microwave hydrothermal process, Zn-Ni-Cr double-layer hydroxides (Zn-Ni-Cr-LDHs) with a surface area of 354 m²/g were created and utilized to remove Cr^{6+} ions from their solution. With an optimal capacity of 28.2 mg/g, the produced adsorbent's suggested function was primarily an electrostatic contact between the Cr^{6+} ion and the adsorbent¹³⁵. Three metal ions, namely Cd^{2+} , Pb^{2+} , and Cu^{2+} , were extracted from the aqueous solutions using Mg-Al-LDH intercalated with sodium alginate (SA-LDH)¹³³. For Cu^{2+} , Pb^{2+} , and Cd^{2+} metal ions, the produced LDH showed optimal capacities at 60 mg/g, 243.7 mg/g, and 95.6 mg/g. Precipitation, substitution, chelation, and bonding or complexation with hydroxyl or oxygen groups at the surface were the suggested functions of the produced LDH.

The lungs, kidneys, and heart are severely harmed by organic chemicals, particularly by benzene and poly-nuclear derivatives including phenol, benzene, toluene, and xylenes. Although these pollutants are found in water in low quantities, their propensity to accumulate in all tissues makes their detrimental effects on the environment quite effective¹³⁶.

The many types of anions present in wastewater, such as sulfates, nitrates, chromates, permanganates, arsenate, phosphates, selenates, and borates, are among the oxygenated anions pollutants. These anions are dangerous to people at low concentrations^{137,138}. Phosphate oxo-anions were adsorbed from their aqueous solution using zirconium-modified Mg-Al-LDH, which were made utilizing the co-precipitation process followed by calcination process to produce the oxide form Zr-LDH¹³⁹. The maximal adsorption capabilities of Zr-LDH and Zr-LDH were found to be 99.5 mg/g and 80.3 mg/g, respectively. A one-pot in-situ hydrothermal approach¹³⁷ was used to manufacture magnesium-aluminum double hydroxides (Mg-Al

View Article Online

DOI: 10.1039/D4YA00272E



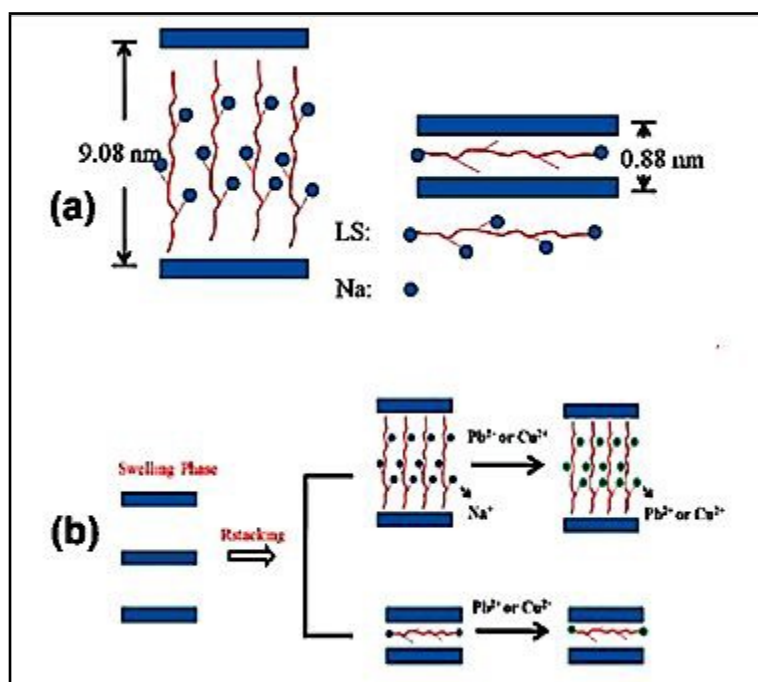
LDHs) to remove arsenate and phosphate oxo-anions from their aqueous solution. Maximum removal capacities for phosphate and arsenate from Mg-Al LDH produced with a 2:1 molar ratio of Mg and Al at 150 °C were found to be 33.2 mg/g and 56.3 mg/g, respectively. It was proposed that the ion exchange process takes place when the nitrate interlayer anions swap arsenate or phosphate anions. However, a coordination mechanism was proposed for mixed anionic solutions. Fe-Mg-Mn-LDH was prepared using the co-precipitation approach¹⁴⁰. Ion exchange and electrostatic attraction were the methods used to remediate the nitrate anions on the manufactured LDH adsorbent. Several mechanisms were reported during the use of LDH in the remediation of environmental contaminants. Physical adsorption: Because the layered double hydroxides have a relatively larger surface area and because their surface contains both positively and negatively adsorptive active sites, physical adsorption has taken place on their surface. Compared to the most well-known conventional adsorbents, they have enhanced adsorption capabilities. The adsorption capacity of the layered double hydroxides (LDH) can be modified by calcining their structures at high temperatures of up to 700 °C to produce their oxide forms.

Ion exchange mechanism: it occurs efficiently in the presence of charged pollutants and results in the swapping of the cations and anions existing in the medium for the structural anions or cations offered in the interlayer network of LDHs. This process may also be linked to the ionic species' chelation via the *d*-transition in the crystalline construction of LDHs.

The adsorption mechanism of the different toxic contaminants on LDH-containing hybrids mainly depends on the type of hybridizing material (adsorbent) and pollutant (adsorbate). Generally, physical adsorption, hydroxide precipitation, anion-metal complexes, electrostatic interaction, π - π interactions, and chemical bonding are the common mechanisms involved in the adsorption process of LDH-containing hybrids¹⁴¹. In Anionic/LDH, the adsorption of heavy metal ions is associated with the formation of anion-metal complexes and hydroxide precipitation on LDH surfaces through chemical bonding with the hydroxyl groups of LDH¹⁴².

Figure 12a-b represents the attachment of Cu^{2+} and Pb^{2+} through an ion-exchange mechanism on the sulfonated lignin (LS)/LDH¹⁴³. Ma et al.¹⁴⁴ studied the adsorption of metal ions on intercalated LDH-containing polysulfide. After the formation of polysulfide-metal complexes, the LDH-containing polysulfide is converted into pristine LDH. The reaction schematic is represented by the following reaction.





View Article Online
DOI: 10.1039/D4YA00272E

Figure 12: Sketch presentation of (a) two existing ways of LS in MgAl/(LDH) interlayer and (b) attachment of Cu^{2+} and Pb^{2+} with LS-LDH

6. Conclusion and Future Directions

Research has shown that the function of anion exchange for LDH may be efficiently regulated by substituting the layers-forming cation. However, they simply pay attention to the phenotypic and morphological descriptions of their structures, and they employ the LDH findings without further investigating and evaluating the function of this mechanism. The function of metal cation coordination in binary or multi-component LDH systems, as well as the change of their crystalline structure, is to govern and regulate the corresponding crystallinity and crystal constructions. However, in Ni-Fe system LDHs, only the coordination interaction among the metal cations has been completely and systematically investigated. The literature in this area is excessively fragmented, and although horizontal and longitudinal comparison experiments are a helpful tactic, no consistent theory has been developed. This gap might be closed by further study. It was discovered that the LDH materials improved with active carbon have not yet undergone enough analysis during the photolysis of newly discovered contaminants and need additional in-depth experimental research in the next subjects.

1. The biomass sources used to prepare the activated carbons that are mixed with LDHs must be varied. There are several biomass sources of carbon nowadays, but investigations suggest that only a few numbers of them can be used to commercially



create LDH composites. Future investigations on the process of producing LDH from biomass carbon are needed.

2. The mechanistic study used to explain how LDH-Carbon composites break down organic contaminants is not exact enough. It is now known that active radicals perform well in photocatalytic decomposition processes; however, it is still unknown how adding carbon elements to composites improves their ability to decompose pollutants and how this affects efficiency or transmission channels. Whether photo-generated electrons are not fully characterized is uncertain. Future studies will focus further on the process by which LDH-C breaks down organic hazardous waste.
3. It is emerging to investigate additional factors for the industrialization of wastewater cleanup; research should be directed toward pilot plants and industrial manufacturing.

Declaration of Competing Interest

The authors declare that they have no conflict of interest .

Acknowledgment

The authors extend their appreciation to Taif University, Saudi Arabia, for supporting this work through the TU-distinguished scientific publishing program and international appearance, Project number (TU-DSPP-2024-265).

References

- [1] P. Kuśtrowski, D. Sułkowska, L. Chmielarz, R. Dziembaj, *Appl. Catal. A Gen.* 302 (2006) 317–324.
- [2] L. Meili, P. V Lins, C.L.P.S. Zanta, J.I. Soletti, L.M.O. Ribeiro, C.B. Dornelas, T.L. Silva, M.G.A. Vieira, *Appl. Clay Sci.* 168 (2019) 11–20.
- [3] P. Lins, D. Henrique, A. Ide, C. Zanta, L. Meili. *Sci. Pollut. Res.* 26 (2019) 31804-31811.
- [4] A. Navajas, I. Campo, A. Moral, J. Echave, O. Sanz, M. Montes, J.A, *Fuel* 211 (2018) 173–181.
- [5] M. Hájek, A. Tomášová, J. Kocík, V. Podzemna, *Appl. Clay Sci.* 154 (2018) 28–35.
- [6] A. Vaccari, *Appl. Clay Sci.* 14 (1999) 161–198.
- [7] G. Hincapié, D. López, A. Moreno, *Catal. Today* 302 (2017).
- [8] H. Griffiths, *Layered Double Hydroxides: Structure, Synthesis and Catalytic Applications*, 2012.
- [9] V. Cunha, A.M. Da Costa Ferreira, V. Constantino, J. Tronto, J. Valim, *Quim. Nova* 33 (2009) 159–171.
- [10] J. Chen, C. Wang, Y. Zhang, Z. Guo, Y. Luo, C.-J. Mao, *Appl. Surf. Sci.* 506 (2019) 144999.



- [11] J. Gonçalves, P. Martins, L. Angnes, K. Araki, *New J. Chem.* 44 (2020).
- [12] A.L. Johnston, E. Lester, O. Williams, R.L. Gomes, *J. Environ. Chem. Eng.* 9 (2021) 105197.
- [13] L. Wu, F.-S. Pan, Y. Liu, G. Zhang, A. Tang, A. Atrens, *Surf. Eng.* 34 (2017) 1–8.
- [14] M.A. Ahmed, A.A. Mohamed, *Inorg. Chem. Commun.* 148 (2023) 110325.
- [15] A. Iqbal, M. Fedel, *Coatings* 9 (2019) 30.
- [16] G.M. Tomboc, T. Kim, S. Jung, H.J. Yoon, K. Lee, *Small* 18 (2022) 1842–1855.
- [17] S. Nayak, K. Parida, *Catalysts* 11 (2021) 1072.
- [18] L.C.D. Agostino, R.G.L. Gonçalves, C.V. Santilli, S.H. Pulcinelli, *Sociedade Brasileira de Pesquisa de Materiais, Brazil*, 2019.
- [19] L. Valeikiene, M. Roshchina, I. Grigoraviciute-Puroniene, V. Prozorovich, A. Zarkov, A. Ivanets, A. Kareiva, *Crystals* 10 (2020) 470.
- [20] A Farhan, A. Khalid, N. Maqsood, S. Iftexhar, H.M.A Sharif, F. Qi, M. Sillanpaa, M.B. Asifi, *Sci. Total Environ.* 912 (2024) 169160.
- [21] L. Čapek, P. Kutálek, L. Smoláková, M. Hájek, I. Troppová, D. Kubička, *Top. Catal.* 56 (2013).
- [22] R. Gabriel, S. Carvalho, J. Duarte, L. Oliveira, D.A. Giannakoudakis, K. Triantafyllidis, J. Soletti, L. Meili, *Appl. Catal. A Gen.* 630 (2021) 118470.
- [23] N. Balsamo, K. Sapag, M. Oliva, G. Pecchi, G. Eimer, M. Crivello, *Catal. Today* 279 (2016).
- [24] R. Yang, Y. Gao, J. Wang, Q. Wang, Layered double hydroxide (LDH) derived catalysts for simultaneous catalytic removal of soot and NOx, *Dalton Trans.* 43 (2014).
- [25] C. Noda Pérez, C.A. Pérez, C.A. Henriques, J.L.F. Monteiro, *Appl. Catal. A Gen.* 272 (2004) 229–240.
- [26] M. Mostafa, M. Betiha, A. Rabie, H. Hassan, A. Morshedy, *Ind. Eng. Chem. Res.* 57 (2017).
- [27] Y.M. Zheng, N. Li, W.-D. Zhang, *Colloids Surfaces A Physicochem. Eng. Asp.* 415 (2012) 195–201.
- [28] R. Shabbir, A. Gu, J. Chen, M. Khan, P. Wang, Y. Jiao, Z. Zhang, Y. Liu, Y. Yang, *Int. J. Environ. Anal. Chem.* 102 (2020) 1–18.
- [29] H. Wang, Q. Fan, Z. Yang, S. Tang, C. Jingye, Y. Wu, *Mol. Catal.* 468 (2019) 1–8.
- [30] E. Musella, I. Gualandi, G. Ferrari, D. Mastroianni, E. Scavetta, M. Giorgetti, A. Migliori, M. Christian, V. Morandi, R. Denecke, M. Gazzano, D. Tonelli, *Electrochim. Acta* 365 (2021) 137294.

View Article Online
DOI: 10.1039/D4YA00272E



- [31] J. Li, L. Yan, Y. Yang, X. Zhang, R. Zhu, H. Yu, *New J. Chem.* 43 (2019) 15915–15923. Article Online
DOI: 10.1039/D4YA00272E
- [32] M. Sousa, F. Tourinho, J. Rubim, *J. Raman Spectrosc.* 31 (2000) 185–191.
- [33] T. Kloprogge, M. Weier, I. Crespo, M. Ulibarri, C. Barriga, V. Rives, W. Martens, R., *J. Solid State Chem.* 177 (2004).
- [34] L. Miranda, C. Bellato, M. Fontes, M. Fabiano de Almeida, J. Milagres, L. Minim, *Chem. Eng. J.* 254 (2014) 88–97.
- [35] C. Hobbs, S. Jaskaniec, E. McCarthy, C. Downing, K. Opelt, K. Güth, A. Shmeliov, M. Mourad, K. Mandel, V. Nicolosi, *Npj 2D Mater. Appl.* 2 (2018).
- [36] F. Dionigi, Z. Zeng, I. Sinev, T. Merzdorf, S. Deshpande, M.B. Lopez, S. Kunze, I. Zegkinoglou, H. Sarodnik, D. Fan, A. Bergmann, J. Drnec, J.F. de Araujo, M. Gliech, D. Teschner, J. Zhu, W.X. Li, J. Greeley, B., *Nat. Commun.* 11 (2020) 1–10.
- [37] A.M. Rabie, E.A. Mohammed, N.A. Negm, *J. Mol. Liq.* 254 (2018) 260–266.
- [38] N.A. Negm, A.M. Rabie, E.A. Mohammed, Molecular interaction of heterogeneous catalyst in catalytic cracking process of vegetable oils: chromatographic and biofuel performance investigation, *Appl. Catal. B Environ.* 239 (2018) 36–45.
- [39] N.A. Negm, G.H. Sayed, F.Z. Yehia, O.I. Habib, E.A. Mohamed, *J. Mol. Liq.* 234 (2017) 157–163.
- [40] N.A. Negm, G.H. Sayed, O.I. Habib, F.Z. Yehia, E.A. Mohamed, *J. Mol. Liq.* 237 (2017) 38–45.
- [41] N.A. Negm, G.H. Sayed, F.Z. Yehia, O.I.H. Dimitry, A.M. Rabie, E.A.M. Azmy, *Egypt. J. Chem.* 59 (2016) 1045–1060.
- [42] H.A. Ahmed, A.A. Altalhi, S.A. Elbanna, H.A. El-Saied, A.A. Farag, N.A. Negm, E.A. Mohamed, *ACS Omega* 7 (2022) 4585–4594.
- [43] A.A. Altalhi, S.M. Morsy, M.T.H. Abou Kana, N.A. Negm, E.A. Mohamed, *Alexandria Eng. J.* 61 (2022) 4847–4861.
- [44] E.A. Mohamed, M.A. Betiha, N.A. Negm, *Energy & Fuels* 37 (2023) 2631–2647.
- [45] S. Ha Lee, S.M. Tawfik, D.T. Thangadurai, Y.-I. Lee, *Microchem. J.* 164 (2021) 106010.
- [46] B.A.A. Balboul, A.A. Abdelrahman, H.M. Salem, E.A. Mohamed, D.I. Osman, A.M. Rabie, *J. Mol. Liq.* 367 (2022) 120562.
- [47] J. Shumaker, C. Crofcheck, S. Tackett, E. Santillan-Jimenez, T. Morgan, Y. Ji, M. Crocker, T. Toops, *Appl. Catal. B-Environmental*, 82 (2008) 101–120.
- [48] N. Bálsamo, S. Mendieta, A. Heredia, M. Crivello, *Mol. Catal.* 481 (2020) 110290.
- [49] D.G. Cantrell, L.J. Gillie, A.F. Lee, K. Wilson, *Appl. Catal. A Gen.* 287 (2005) 183–190.
- [50] P.-L. Boey, G.P. Maniam, S. Hamid, *Bioresour. Technol.* 100 (2009) 6362–6368.



- [51] S. Sankaranarayanan, C.A. Antonyraj, S. Kannan, *Bioresour. Technol.* 109 (2012) 57–62. View Article Online
DOI: 10.1039/D4YA00272E
- [52] R. Prado, G. Almeida, M. Carvalho, L. Galvao, C. Cardoso Bejan, L. Costa, F. Pinto, J. Tronto, D. Pasa, *Catal. Letters* 144 (2014) 1062–1073.
- [53] S. Yan, S.O. Salley, K.Y. Simon Ng, *Appl. Catal. A Gen.* 353 (2009) 203–212.
- [54] T. Montanari, M. Sisani, M. Nocchetti, R. Vivani, C. Herrera, G. Ramis, G. Busca, U. Costantino, *Catal. Today*, 152 (2010) 104–109.
- [55] R. Gabriel, S.H.V. de Carvalho, J.L.S. Duarte, L.M.T. Oliveira, D.A. Giannakoudakis, K.S. Triantafyllidis, J.I. Soletti, L. Meili, *Appl. Catal. A: General* 630 (2022) 118470.
- [56] L. Fereidooni, A. Pirkarami, E. Ghasemi, A. Kasaeian, *Energy Convers. Manag.* 296 (2023) 117646.
- [57] G. Arzamendi, E. Arguiñarena, I. Campo, S. Zabala, L.M. Gandía, *Catal. Today* 135 (2008) 305–313.
- [58] D. Wang, X. Zhang, C. Liu, T. Cheng, W. Wei, Y. Sun, *Appl. Catal. A Gen.* 505 (2015) 478–486.
- [59] A. Stamate, O.D. Pavel, R. Zavoianu, *Catalysts* 10 (2020) 57.
- [60] C. Kajdas, *Lubr. Sci.* 6 (1994) 203–228.
- [61] Y. Wang, M. Zhang, Y. Liu, Z. Zheng, B. Liu, M. Chen, G. Guan, K. Yan, *Adv. Sci.* 10 (2023) 1–28..
- [62] K. Yan, Y. Liu, Y. Lu, J. Chai, L. Sun, *Catal. Sci. Technol.* 7 (2017) 1622–1645.
- [63] M. Zhang, Y. Liu, B. Liu, Z. Chen, H. Xu, K. Yan, *ACS Catal.* 10 (2020) 5179–5189.
- [64] J. Zhang, J. Sun, Y. Wang, *Green Chem.* 22 (2020) 1072–1098.
- [65] Y. Zeng, L. Lin, D. Hu, Z. Jiang, S. Saeed, R. Guo, I. Ashour, K. Yan, *Catal. Today* 423 (2023) 114252.
- [66] V. Rives, D. Carriazo, C. Martin, In book: *Pillared clays and related catalysts*, 12 (2010) 319–397.
- [67] X. Wang, C. Shang, G. Wu, X. Liu, H. Liu, *Catalysts* 6 (2016).
- [68] J. C. Manayil, S. Sankaranarayanan, D. Bhadoria, K. Srinivasan, *Ind. Eng. Chem. Res.* 50 (2011) 13380–13386.
- [69] G. Wu, X. Wang, J. Li, N. Zhao, Y. Sun, *Catal. Today* 131 (2008) 402–407.
- [70] L.S. Randarevich, I.Z. Zhuravlev, V. V. Strelko, N.M. Patrilyak, T.A. Shaposhnikova, J. Water Chem. Technol. 31 (2009) 110–114.
- [71] A. Tsyganok, R.G. Green, J.B. Giorgi, A. Sayari, *Catal. Commun.* 8 (2007) 2186–2193.
- [72] F. Malherbe, C. Depège, C. Forano, J.P. Besse, M.P. Atkins, B. Sharma, S.R. Wade, *Appl. Clay Sci.* 13 (1998) 451–466.



- [73] A.L. Villa, D.E. De Vos, F. Verpoort, B.F. Sels, P.A. Jacobs, *J. Catal.* 198 (2001) 223–231. Article Online
DOI: 10.1039/D4YA00272E
- [74] A. Maciucă, E. Dumitriu, F. Fajula, V. Hulea, *APPL CATAL A-GEN* 338 (2008) 1–8.
- [75] H.D. Smith, G.M. Parkinson, R.D. Hart, *J. Cryst. Growth* 275 (2005) 1665–1671.
- [76] S. Soled, D. Levin, S. Miseo, J. Ying, *Prep. Catal. VII*, Elsevier, 1998: pp. 359–367.
- [77] J. Zhao, J. Liu, Q. Han, L. Chen, *Cryst. Eng. Comm.* 18 (2016).
- [78] M. Del Arco, D. Carriazo, S. Gutiérrez, C. Martín, V. Rives, *Inorg. Chem.* 43 (2004)
- [79] B.M. Choudary, T. Someshwar, C.V. Reddy, M.L. Kantam, K.J. Ratnam, L. V Sivaji, *Appl. Catal. A Gen.* 251 (2003) 397–409.
- [80] B. Sels, D. De Vos, M. Buntinx, F. Plerard, A. Kirsch-De Mesmaeker, P. Jacobs, *Nature* 400 (1999) 855–857.
- [81] J. Palomeque, F. Figueras, G. Gelbard, *Appl. Catal. A Gen.* 300 (2006) 100–108.
- [82] D. Carriazo, S. Lima, C. Martín, M. Pillinger, A.A. Valente, V. Rives, *J. Phys. Chem. Solids* 68 (2007) 1872–1880.
- [83] Y. Hanifah, R. Mohadi, M. Mardiyanto, A. Lesbani, *Ecol. Eng. Environ. Technol.* 24 (2023) 109–116.
- [84] B. Zeynizadeh, M. Gilanizadeh, *New J. Chem.* 43 (2019) 18794–18804.
- [85] E. Stamate, O.D. Pavel, R. Zăvoianu, B. Ioana, A. Ciorîță, R. Birjega, K. Neubauer, A. Köckritz, *I.C. Materials (Basel)*. 14 (2021) 7457.
- [86] N. Ahmed, R. Menzel, Y. Wang, A. García, S. Bawaked, A. Obaid, S. Basahel, M. Mostafa, *J. Solid State Chem.* 246 (2016).
- [87] M. García Álvarez, D. Crivoi, F. Medina, D. Tichit, *ChemEngineering* 3 (2019).
- [88] N. Ma, Y. Song, F. Han, G. Waterhouse, Y. Li, S. Ai, *Catal. Sci. Technol.* 10 (2020).
- [89] S. Xia, L. Zheng, W. Ning, L. Wang, P. Chen, Z. Hou, , *J. Mater. Chem. A*. 1 (2013).
- [90] Y. Yang, W. Zhu, D. Cui, C. Lü, *Appl. Clay Sci.* 200 (2021) 105958.
- [91] D. Tichit, G. Layrac, C. Gerardin, *Chem. Eng. J.* 369 (2019).
- [92] Z. Georgiopoulou, A. Verykios, K. Ladomenou, K. Maskanaki, G. Chatzigiannakis, K.-K. Armadorou, L. Palilis, A. Chroneos, S. Gardelis, A. Yusoff, T. Coutsolelos, K. Aidinis, M. Vasilopoulou, A. Soultati, *Nanomaterials* 13 (2022) 169.
- [93] G. Fan, D. Evans, X. Duan, *Chem. Soc. Rev.* 43 (2014).
- [94] X. Wu, Y. Du, X. An, X. Xie, *Catal. Commun.* 50 (2014) 44–48.
- [95] Z. Wang, C. Li, K. Domen, *Chem. Soc. Rev.* 48 (2019) 2109–2125.
- [96] J.S. Schubert, J. Popovic, G.M. Haselmann, S.P. Nandan, J. Wang, A. Giesriegl, A. S. Cherevan, D. Eder, *J. Mater. Chem. A* 7 (2019) 18568–18579.



- [97] S.F. Ng, M.Y.L. Lau, W.J. Ong, *Sol. RRL* (2021) 2000535.
- [98] Y. Zhao, G.I.N. Waterhouse, G. Chen, X. Xiong, L.-Z. Wu, C.-H. Tung, T. Zhang, *Chem. Soc. Rev.* 48 (2019) 1972–2010
- [99] H. Boumeriame, E.S. Da Silva, A.S. Cherevan, T. Chafik, J.L. Faria, D. Eder, J. Energy Chem. 64 (2022) 406–431.
- [100] Y. Wang, Y. Zhang, Z. Liu, C. Xie, S. Feng, D. Liu, M. Shao, S. Wang, *Angew. Chem. Int. Ed.* 56 (2017) 5867.
- [101] S. Dou, L. Tao, R. Wang, S. E. Hankari, R. Chen, S. Wang, *Adv. Mater.* 30 (2018) 1705850.
- [102] Y. Zhao, G. Waterhouse, G. Chen, X. Xiong, L.-Z. Wu, C.-H. Tung, T. Zhang, *Chem. Soc. Rev.* 48 (2018).
- [103] X. Sun, L. Shi, H. Huang, X. Song, T. Ma, *Chem. Commun.* 56 (2020) 11000–11013.
- [104] X. Lu, H. Xue, H. Gong, M. Bai, D.-M. Tang, R. Ma, T, *Nano-Micro Lett.* 12 (2020).
- [105] D. Tang, J. Liu, X. Wu, R. Liu, X. Han, Y. Han, H. Huang, Y. Liu, Z.H. Kang, *ACS Appl. Mater. Interfaces* 6 (2014).
- [106] W. Ma, R. Ma, C. Wang, J. Liang, X. Liu, K. Zhou, T. Sasaki, *ACS Nano* 9 (2015).
- [107] G. Shi, C. Yu, Z. Fan, J. Li, M. Yuan, *ACS Appl. Mater. Interfaces* 11 (2018).
- [108] T. Bhowmik, M. Kundu, S. Barman, *ACS Appl. Energy Mater.* 1 (2018).
- [109] L. Yipu, X. Liang, L. Gu, Y. Zhang, G.-D. Li, X. Zou, J. Chen, *Nat. Commun.* 9 (2018).
- [110] Z. Yan, H. Sun, X. Chen, H. Liu, Y. Zhao, H. Li, W. Xie, F. Cheng, J. Chen, *Nat. Commun.* 9 (2018).
- [111] X. Lu, C. Zhao, *Nat. Commun.* 6 (2015) 6616.
- [112] W. Qichen, X.-X. Xue, Y. Wang, Y. Feng, X. Xiong, D. Wang, Y. Li, *Small* 16 (2020).
- [113] T. Ling, T. Zhang, B. Ge, L. Han, L. Zheng, F. Lin, Z. Xu, W. Hu, X. Du, K. Davey, S. Qiao, *Adv. Mater.* 31 (2019) 1807771.
- [114] F. Guozhao, W. Qichen, J. Zhou, Z. Chen, Z. Wang, A. Pan, S. Liang, *ACS Nano* 13 (2019).
- [115] J.F. Qin, M. Yang, T.S. Chen, B. Dong, S. Hou, X. Ma, Y.N. Zhou, X.L. Yang, J. Nan, Y.M. Chai, *Int. J. Hydrogen Energy* 45 (2019).
- [116] C. Lei, W. Zhou, Q. Feng, Y. Zhang, Y. Chen, J. Qin, *Nano-Micro Lett.* 11 (2019) 45.
- [117] R. li, J. Wang, B. Zhou, M.K. Awasthi, A. Ali, Z. Zhang, L. Gaston, A. Lahori, D.A. Mahar, J. Gan, *Sci. Total Environ.* 559 (2016) 121–129.
- [118] Y. Yang, W. Zhang, Y. Xiao, Z. Shi, X. Cao, Y. Tang, Q. Gao, *Appl. Catal. B Environ.* 242 (2018).

View Article Online
DOI: 10.1039/D4YA00272E



- [119] H. Liang, A.N. Gandi, C. Xia, M.N. Hedhili, D.H. Anjum, U. Schwingenschlög, H.N. Alshareef, *ACS Energy Lett.* 2 (2017) 1035–1042. Article Online
DOI: 10.1039/D4YA00272E
- [120] K. He, T. Tsega, X. Liu, J. Zai, X.-H. Li, X. Liu, W. Li, N. Ali, X. Qian, *Angew. Chemie Int. Ed.* 58 (2019).
- [121] H. Zhang, X. Li, A. Hähnel, V. Naumann, C. Lin, S. Azimi, S. Schweizer, W. Maijenburg, R. Wehrspohn, *Adv. Funct. Mater.* 28 (2018) 1706847.
- [122] M.N. Nimbalkar, B.R. Bhat, *J. Environ. Chem. Eng.* 9 (2021) 106216.
- [123] A. Yadav, N. Bagotia, A. Sharma, S. Kumar, *Sci. Total Environ.* 784 (2021) 147108.
- [124] A. Yadav, N. Bagotia, A. Sharma, S. Kumar, *Sci. Total Environ.* 799 (2021) 149500.
- [125] D. Ahmed, L. Najj, A. Faisal, N. Al-Ansari, M. Naushad, *Sci. Rep.* 10 (2020).
- [126] A. Farhan, J. Arshad, E.U. Rashid, H. Ahmad, S. Nawaz, J. Munawar, J. Zdarta, T. Jesionowski, M. Bilal, *Chemosphere* 310 (2023) 136835.
- [127] M. El-Abboubi, N. Taoufik, F. Kzaiber, N. Barka, F.Z. Mahjoubi, O. Abdelkhalek, Sorption of methyl orange dye by dodecyl-sulfate intercalated Mg-Al layered double hydroxides, *Mater. Today Proc.* 37 (2020).
- [128] M. Kostić, S. Najdanović, N. Velinov, M. Radović Vučić, M. Petrović, J. Mitrović, A. Bojić, *Environ. Technol. Innov.* 26 (2022) 102358.
- [129] M. Mureseanu, A. Eliescu, E.C. Ignat, G. Carja, N. Cioatera, *Comptes Rendus Chim.* 25 (2022).
- [130] R. Gayathri, G. Kannappan Panchamoorthy, P. Kumar, *Chemosphere* 262 (2020).
- [131] A. Amer, G.H. Sayed, R.M. Ramadan, A.M. Rabie, N.A. Negm, A.A. Farag, E.A., *J. Mol. Liq.* 341 (2021) 116935.
- [132] M.R. Pérez, I. Pavlovic, C. Barriga, J. Cornejo, M.C. Hermosín, M.A. Ulibarri, *Appl. Clay Sci.* 32 (2006) 245–251.
- [133] X. Zhang, R. Shan, X. Li, L. Yan, Z. Ma, R. Jia, S. Sun, *Water Sci. Technol.* 83 (2021).
- [134] M. Dinari, S. Neamati. *Eng. Asp.* 589 (2020) 124438.
- [135] L. Guo, Y. Zhang, J. Zheng, L. Shang, Y. Shi, Q. Wu, X. Liu, Y. Wang, L. Shi, Q. Shao, *Adv. Compos. Hybrid Mater.* 4 (2021) 1–11.
- [136] S. Somma, E. Reverchon, L. Baldino, *Chem. Engineering* 5 (2021) 47.
- [137] K.W. Jung, S.Y. Lee, J.W. Choi, M.J. Hwang, W.G. Shim, *Chem. Eng. J.* 420 (2021) 129775.
- [138] S. Li, X. Ma, Z. Ma, X. Dong, Z. Wei, X. Liu, L. zhu, *Environ. Technol. Innov.* 23 (2021) 101771.
- [139] M. Motandi, Z. Zhang, I. Stelgen, L. Yan, *Environ. Prog. Sustain. Energy* 41 (2021).



- [140] H. Zhou, Y. Tan, W. Gao, Y. Zhang, Y. Yang, *Sci. Rep.* 10 (2020) 16126. View Article Online
DOI: 10.1039/D4YA00272E
- [141] L. Tan, Y. Wang, Q. Liu, J. Wang, X. Jing, L. Liu, J. Liu, D. Song, , *Chem. Eng. J.* 259 (2015) 752–760.
- [142] N. Wang, J. Sun, H. Fan, S. Ai, *Talanta* 148 (2016) 301–307.
- [143] G. Huang, D. Wang, S. Ma, J. Chen, L. Jiang, P. Wang, *J. Colloid Interface Sci.* 445 (2015) 294–302.
- [144] S. Ma, Q. Chen, H. Li, P. Wang, S.M. Islam, Q. Gu, X. Yang, M.G. Kanatzidis, *J. Mater. Chem. A* 2 (2014) 10280–10289.



No primary research results, software or code have been included and no new data were generated or analysed as part of this review.

